



1N-26  
381 818

# TECHNICAL NOTE

## D-6

VACUUM-INDUCTION, VACUUM-ARC, AND AIR-INDUCTION  
MELTING OF A COMPLEX HEAT-RESISTANT ALLOY

By R. F. Decker, John P. Rowe, and J. W. Freeman

University of Michigan

NATIONAL AERONAUTICS AND SPACE ADMINISTRATION  
WASHINGTON

August 1959



NATIONAL AERONAUTICS AND SPACE ADMINISTRATION

TECHNICAL NOTE D-6

VACUUM-INDUCTION, VACUUM-ARC, AND AIR-INDUCTION

MELTING OF A COMPLEX HEAT-RESISTANT ALLOY

By R. F. Decker, John P. Rowe, and J. W. Freeman

SUMMARY

The relative hot-workability and creep-rupture properties at 1,600° F of a complex 55Ni-20Cr-15Co-4Mo-3Ti-3Al alloy were evaluated for vacuum-induction, vacuum-arc, and air-induction melting. A limited study of the role of oxygen and nitrogen and the structural effects in the alloy associated with the melting process was carried out.

The results showed that the level of boron and/or zirconium was far more influential on properties than the melting method. Vacuum melting did reduce corner cracking and improve surface during hot-rolling. It also resulted in more uniform properties within heats. The creep-rupture properties were slightly superior in vacuum heats at low boron plus zirconium or in heats with zirconium. There was little advantage at high boron levels and air heats were superior at high levels of boron plus zirconium. Vacuum heats also had fewer oxide and carbonitride inclusions although this was a function of the opportunity for separation of the inclusions from high oxygen plus nitrogen heats. The removal of phosphorous by vacuum melting was not found to be related to properties.

Oxygen plus nitrogen appeared to increase ductility in creep-rupture tests suggesting that vacuum melting removes unidentified elements detrimental to ductility. Oxides and carbonitrides in themselves did not initiate microcracks. Carbonitrides in the grain boundaries of air heats did initiate microcracks. The role of microcracking from this source and as a function of oxygen and nitrogen content was not clear. Oxygen and nitrogen did intensify corner cracking during hot-rolling but were not responsible for poor surface which resulted from rolling heats melted in air.

INTRODUCTION

Variations in creep-rupture properties among heats of an alloy of constant nominal composition have been characteristic of heat-resistant alloys. Many of these variations have been attributed to prior-history

effects from melting operations. The objective of this program was to establish the role of several melting variables in heat-to-heat variations. Furthermore, it was desired that mechanisms be established to obtain the basic knowledge necessary for melt control to yield reproducible heat-to-heat creep-rupture properties.

Early research on this program was restricted to vacuum-induction melting. It was found (ref. 1) that a major source of heat-to-heat variations was the boron and/or zirconium content of the heats, either from "deoxidants," added inadvertently from crucible contamination of the melt or unknowingly from the melting stock. The program herein described was designed to broaden the scope of the melting practices to include vacuum-arc melting in a cold mold and air-induction melting.

Boron and zirconium were varied to allow comparison of melting methods on materials of comparable levels of these influential elements. A melting technique was developed to permit additions of oxygen, nitrogen, and phosphorous after vacuum melting. This technique was designed to correlate property effects with effects of melting practice on chemistry. Finally, a limited correlation of microstructures with properties and chemistry was made to obtain further basic mechanistic information.

The assistance of Messrs. K. E. Kienholz, T. M. Cullen, J. E. Wells, A. G. Dano, R. Umstead, T. Spence, and G. Hynes, Miss Christine Sadler and Mrs. Geraldine Andrews was most helpful in various portions of the experimental work. This investigation was conducted at the University of Michigan under the sponsorship and with the financial assistance of the National Advisory Committee for Aeronautics.

## EXPERIMENTAL PROCEDURES

### Melting

Aim analysis for the basic constituents of the alloy was as follows, in weight percent:

<u>Cr</u>	<u>Co</u>	<u>Mo</u>	<u>Ti</u>	<u>Al</u>	<u>Si</u>	<u>Mn</u>	<u>C</u>	<u>Ni</u>
20.0	15.0	4.0	3.1	3.1	0.12	0.12	0.08-.15	Bal.

Varied amounts of boron, zirconium, oxygen, nitrogen, and phosphorous were added to certain heats for purposes of the investigation.

The melting stock used and analyses reported by manufacturers were:

Nickel - Laboratory grade electrolytic  
Ni - 99.95, Co - .01, Fe - .01-.04, Cu - .01-.03,  
Si and S - trace

Chromium - Laboratory grade electrolytic  
Cr - 99.2, Fe - .09, S - .026, C - .01, Cu - .01,  
Pb - .001, O - .46, N - .026

- Aluminum reduced  
Cr - 99.4, Fe - .28, Si - .11, Al - .06, C - .05,  
S - .025, O - .02, N - .01

Cobalt - Laboratory grade electrolytic  
Co - 99.5+, Ni - .45, Cu - .005, C - .01 - .02,  
Fe - .001, S - .001, Pb - .0001, Zr and As-trace

Molybdenum - Vacuum-arc - cast  
C - .01

Titanium - Ti 55A alloy

Aluminum - Laboratory grade ingot  
Al - 99.99+, Zn - .005, Fe - .001, Si - .001

Silicon - Purified laboratory grade  
Si - 99.9

Manganese - Laboratory grade electrolytic  
Mn - 99.9+

Carbon - Powdered AUC grade  
C - 99.9, S - .006, P - trace

- Chromium carbide  
C - 9.84, Cr - 89.31, Fe - .45, Si - .05

Boron - Nickel boride

Zirconium - Sponge  
O - .10, N - .08

Nitrogen - Chromium nitride

Oxygen - Nickelous oxide, reagent grade

Phosphorous - Iron phosphide

For all heats nickel, chromium, cobalt, and carbon were melted down in the base charge, followed by additions of molybdenum, silicon, aluminum, titanium, manganese, and boron and zirconium if these latter two elements were being added. Heats designated as V-11 to V-25 were vacuum-induction melted in alumina or magnesia crucibles in the University of Michigan vacuum-melting unit (fig. 1). Pressures before power application, after meltdown, and after pouring were less than 10 microns as measured by both Stokes and thermocouple gages. The air heats, A-1 through A-6, were induction melted at 1 atmosphere while fully exposed to air.

In order to study further the role of oxygen, nitrogen, and phosphorous heats V + Arg-1 through V + Arg-12 were vacuum-induction melted under the same conditions used in the aforementioned vacuum heats. Near the end of the melting cycle, tank argon was admitted up to 400 millimeter pressure, and then additions of N, O, or P were made. The argon helped retain the additions in the heats. In heats V + Arg-1 through V + Arg-9, the argon was admitted at the very end of the melting cycle after aluminum, titanium, boron, and manganese had been added. However, in heats V + Arg-10 through V + Arg-12, argon was admitted and additions of N and O, if any, were made prior to aluminum, titanium, boron, and manganese additions. In one heat the chamber was opened to the air for 15 minutes after vacuum melting before pouring the ingot.

All of the heats weighed ten pounds and were cast in an open-bottomed copper mold which rested on a massive copper block. An insulating refractory ring mounted in the top of the copper mold served as the hot top.

The vacuum-arc cold mold heat was melted gratis by Mallory-Sharon Metals Corp. through the courtesy of Dr. L. S. Busch. The melting stock was machined or pulverized to small particle size and melted into 600 gram buttons in a nonconsumable-electrode button furnace under a positive pressure of argon. The buttons were welded together to form a 16-inch long consumable electrode. This electrode was melted into a 4-inch diameter ingot by consumable-DC arc melting in a water-cooled copper mold. The pressure averaged 13 microns and the leak-up rate before melting was 6 microns per minute. The ingot was quartered, welded to form a second electrode, and remelted into a second 4-inch ingot in the same manner described above. Leak-up rate on this remelt was 1 micron per minute before melting; pressure ranged between 3 and 7 microns during melting.

#### Hot-Working and Heat Treating

The early heats in the investigation, V-11 through 17 and A-2, were homogenized 1 hour at 2,300° F and air-cooled prior to working.

Subsequently, this treatment was found to have no effect on materials with low boron, and was believed to contribute to hot shortness of heats with relatively high boron plus zirconium. Therefore, it was omitted for the other experimental heats.

The majority of the ingots were rolled from 2,150° F to 7/8-inch bar stock using 22 passes with 21 reheats of 10 minutes between passes. The exceptions were heats V-25, A-3, and A-4, which were rolled from 2,000° F using 36 passes with 35 reheats to prevent internal cracking resulting from the relatively high boron plus zirconium in these heats. In all cases, the last reduction of area by rolling was about 10 percent followed by air-cooling. Hot-workability was evaluated by qualitative comparisons of surface cracking after rolling.

All stock was quartered and then heat treated 2 hours at 2,150° F and air-cooled. Aging prior to creep-rupture testing and stress aging occurred during a 4-hour preheat at 1,600° F in the creep-rupture units.

#### Chemical Analysis

Samples for chemical analysis were cut from the midpoint of the as-rolled bar stock, from metal which was at the center of the ingot.

Spectrographic and wet chemical analysis: Chromium, cobalt, molybdenum, titanium, aluminum, manganese, silicon, magnesium, calcium, lead, copper, and iron were determined spectrographically through the courtesy of Utica Drop Forge and Tool Division of Kelsey-Hayes Co.

Boron and zirconium were analyzed spectrographically and/or wet chemically through the courtesy of Universal-Cyclops Steel Corp. and Utica Drop Forge and Tool Division of Kelsey-Hayes Co.

Wet-chemical analyses of carbon and phosphorous, spectrographic analysis of lead and magnesium, and qualitative spectrographic analyses of condensate from the melt were performed at a commercial laboratory. In addition, spectrographic determinations on air and vacuum melted materials were run to detect trace elements other than those listed above.

Sulfur analyses were supplied gratis by Universal-Cyclops Steel Corp.

Vacuum-fusion and Kjeldahl analysis: Vacuum-fusion analyses for oxygen and nitrogen were run at the University of Michigan using the platinum-bath technique of Wilkins and Fleischer (ref. 2). It was easily possible to run 15 1-gram samples during a normal 40-hour week using one bath of 25 grams of platinum.

Since standards for oxygen and nitrogen in this type of alloy were lacking, samples of 18Cr-8Ni stainless steel were obtained gratis from Prof. N. J. Grant of the Massachusetts Institute of Technology. A satisfactory check was obtained as follows:

<u>Source of data</u>	<u>O, (weight, percent)</u>	<u>N, (weight, percent)</u>
M.I.T.	0.029	0.029
U.M. Vacuum Fusion	.023	.029
	.024	.031

In general, blanks did not vary significantly either in one day's run or from day to day. The considerable number of duplicates that were run indicate that good reproducibility was obtained from run-to-run and from beginning to end of one run. In the heats with low gas content, the range of values in one heat for oxygen was less than 0.001 percent and for nitrogen was less than 0.003 percent. However, because of segregation of oxides and nitrides in the bar stock and the necessity for using relatively small samples, the reproducibility was somewhat lower in heats with high oxygen and nitrogen content.

As a further check on the nitrogen analyses obtained by vacuum fusion, micro-Kjeldahl analyses were run in the University of Michigan gas analysis laboratory using the techniques of Hague, Paulson, and Bright (ref. 3). At gas levels below 0.010 N, the maximum range in duplicate samples was 0.005 percent. Although this range increased with nitrogen content, it was usually less than 0.01 percent. The results of these analyses, however, showed that the micro-Kjeldahl values were consistently lower than those obtained by vacuum fusion.

In an effort to ascertain which of the two techniques was yielding the more accurate results, analyses were run on National Bureau of Standards standard sample 169 of 77Ni-20Cr alloy using the micro-Kjeldahl technique. The results were as follows:

<u>Source of Data</u>	<u>N, (weight, percent)</u>
NBS	0.031
U.M. micro-	0.012
Kjeldahl	0.013
	0.016

The cause for this lack of agreement was not identified in spite of repeated modifications in technique to attempt the release of more nitrogen. It was noted, however, that the magnitude of the error indicated



by these checks was of the same order as the differences between the vacuum-fusion results and the micro-Kjeldahl values on the experimental materials. This fact adds credence to the vacuum-fusion data which had been previously shown to give good nitrogen results for 18Cr-8Ni stainless steel. It was, therefore, decided to use the vacuum-fusion results for the property correlations.

### Creep-Rupture Testing and Stress Aging

The creep-rupture properties were evaluated by tests at 1,600° F and 25,000 psi.

The testing and stress aging at 1,600° F were accomplished in creep-rupture units with 0.250-inch test specimens of 1-inch gage section using a 4-hour preheat before load application; creep strain was measured by an optical extensometer system with a sensitivity of 0.000005 inch per inch. Stress aging was designed to give equal strain in equal time at 1,600° F by appropriate stress selection. The specimens were then interrupted by release of the load and immediate removal from the furnace.

### Microstructural Studies

Hardness: Diamond pyramid hardness (DPH) was measured with a 50-kilogram load. Three impressions were made on each sample, both diagonals of each impression being measured. Statistical analysis of testing variability established that a hardness difference of 8 DPH was significant.

Light microscopy: Metallographic samples were mechanically polished through wet papers to 600 grit and then electropolished in a solution of 10 parts of perchloric acid (70 percent) and 90 parts of glacial acetic acid at 50 volts with a current density of 2 amperes per square inch. Cyclic polishing of 5 seconds on and 5 seconds off was employed for a total period of electrolysis of 30 seconds.

The procedure and etchant developed by Bigelow, Amy, and Brockway (ref. 4) was used to best reveal the precipitating phases at 100 and 1,000 diameters. This involved etching electrolytically at 6 volts and a current density of 0.8 ampere per square inch for periods of 5 to 7 seconds, depending upon the sample condition. The etchant composition was 12 parts of phosphoric acid (85 percent), 47 parts of sulfuric acid (96 percent), and 41 parts of nitric acid (70 percent).

Electron microscopy: Metallographic samples were mechanically polished through wet papers to 600 grit. This was followed by electropolishing using the procedure described in the previous section on light microscopy.

Etching for examination with the electron microscope was accomplished with the etchant described under light microscopy with the etching time reduced to periods of 1 to 5 seconds.

After etching, collodion replicas of the metallic surface were made. These were shadowed with palladium to increase contrast and reveal surface contours. Polystyrene latex spheres approximately  $3,400^{\circ}$  angstrom units in diameter were placed on the replicas prior to shadowing to indicate the angle and direction of shadowing and to provide an internal standard for measurement of magnification. The micrographs reproduced in this report are copies of direct prints from the original negatives; consequently, the polystyrene spheres appear black and the "shadows" formed by the palladium appear white.

Counting techniques: In order to make the trends and comparisons quantitative, counts were made of the number of depleted grain boundaries, microcracks, and nodules in an 0.008 square-inch area using a magnification of X1,000 on mechanically polished and etched specimens. An area of 0.008 square inch was surveyed as eight strips, each 0.2 inch by 0.005 inch and longitudinal to the specimen axis at the center of the specimen and at the minimum cross section. A depleted grain boundary was counted when a clear, white strip of matrix free of  $\gamma'$  particles was clearly seen along a grain boundary. Microcracks were easily distinguishable by their blackness which was in complete contrast to all other intragranular and intergranular features of the samples. Early doubts about the identity of microcracks were eliminated when electropolishing enlarged and accentuated these black voids and when fins on electron microscope replicas were found where these had filled the microcracks. Each distinct microcrack was counted. A crack had to be 1 micron in length to be counted because shorter microcracks were not distinguishable from carbide-matrix interfaces. Counting of nodules was limited to those more than 5 microns in diameter.

A rough measure of  $\gamma'$  dispersion was obtained by the surface density of  $\gamma'$  particles in electron micrographs. An area large enough to contain at least 100 particles was surveyed at 12,000 diameters.

The above techniques allow quantitative comparison of the tendency of the heats to undergo structural changes.

## RESULTS

In reference 1 it was shown that the major variables controlling hot-workability and creep-rupture properties of vacuum-induction melted heats of the experimental alloy were boron, zirconium, or boron plus zirconium content. This was true whether these elements were derived

from reaction between the melt and crucible refractories, unknowingly introduced with the raw materials, or added to the heats. Accordingly, the evaluations of the effects of the melting methods investigated for this report had to take into account the influence of these elements.

The evaluation of melting methods was based on cracking during hot-rolling (fig. 2) and creep-rupture properties at 1,600° F and 25,000 psi (figs. 3 through 8) as a function of boron, zirconium, or boron plus zirconium contents of the heats. Duplicate creep-rupture tests were conducted and the average values plotted for each heat.

While the properties have been evaluated in the figures on the basis of boron, zirconium, or boron plus zirconium contents, the oxygen and nitrogen contents were the main variables studied in this investigation. Consequently, the effects were also evaluated in terms of these elements. Vacuum melting also reduced phosphorous content and this element was given special attention for this reason.

The results of chemical analyses for the major elements considered are given in table I. Selected heats, when analyzed for trace amounts of magnesium, calcium, lead, and sulphur did not show significant differences (table II). Table III gives the results of semiquantitative spectrographic analyses of vaporized elements condensed on a cold plate suspended over a melt during vacuum melting. The test data from the creep-rupture tests are given in table IV. This table indicates the tests which were interrupted before fracture to provide specimens for study of structural effects.

Microstructural studies on selected key heats were used to study the mechanism of the melting effects on creep-rupture properties.

### Vacuum-Induction Melting

The basic properties of vacuum-induction heats of the alloy were taken from reference 1 to serve as a base for comparison in evaluating the melting practices studied for this investigation. The curves of figures 3 through 8 are the same as those in reference 1. The only exception was the minimum creep rates in figure 5 which had not been reported previously. These figures express the creep-rupture properties at 1,600° F and 25,000 psi as a function of boron, zirconium, or boron plus zirconium contents.

The creep-rupture test data in table IV include results of rupture tests on vacuum-induction heats V-11 through V-21 from reference 1. These are supplemented by creep data for these heats. The complete rupture and creep data are included for these heats because the creep data are reported for the first time and because the heats had been analyzed

for oxygen and nitrogen. The test data for the vacuum-induction heats involving zirconium or zirconium plus boron from reference 1 are not included in table IV. The average property values are however shown in figures 6, 7, and 8. Figure 6 shows two basic curves for rupture time as influenced by zirconium because there appeared to be slightly longer rupture times for those heats with more than 6.5 percent of titanium plus aluminum (data from ref. 1).

Chemical analyses of heats indicated that vacuum melting influenced the nitrogen, oxygen, and phosphorous contents. The ranges in these elements from table I for vacuum-induction melted heats were as follows:

<u>N,</u> <u>(weight, percent)</u>	<u>O,</u> <u>(weight, percent)</u>	<u>P,</u> <u>(weight, percent)</u>
<0.001 to 0.002	0.0013 to 0.0037	0.004 to 0.008

Since there were very few points on the correlation between rupture properties and zirconium in the presence of boron (fig. 8), heat V-25 was prepared to add another point to this correlation at an intermediate zirconium content. The properties of this heat agreed well with those indicated by the data from reference 1.

In reference 1 it was shown that vacuum heats without boron or zirconium corner cracked during hot-rolling. This was reduced by adding boron as can be seen by comparing photographs of stock from heat V-15 (fig. 2(a)) with that of heat V-12 (fig. 2(b)). Heat V-25 (fig. 2(c)) with boron plus zirconium was also free from corner cracking. It was, however, necessary to reduce the rolling temperature and amount of reduction to prevent center cracking in the heat containing both boron and zirconium. Zirconium alone reduced corner cracking but was not nearly as effective as boron.

This background of information provided by the data of reference 1, and summarized above, served as the basis for evaluation of melting practice variables in the present investigation.

#### Vacuum-Arc Melting in Cold Mold

Due to unknown reasons the heat melted by the consumable-electrode vacuum-arc cold-mold method (heat V-Arc) had slightly higher boron (0.0006 percent) and slightly higher zirconium (0.015 percent) than the vacuum-induction heats melted in alumina without deliberate additions. For this reason no applicable data for comparison at the same level of both boron and zirconium are available for induction heats. The rupture time was slightly on the low side for the boron content (fig. 3) while the ductility and creep rate were somewhat high (figs. 4 and 5). The

strength and ductility were both slightly higher than for the lower boron, zirconium heats (figs. 6 and 7). In general, the properties are quite close to those which would be expected for vacuum-induction heats with approximately the same boron and zirconium contents.

The heat showed considerable corner cracking during hot-working (fig. 2(d)). The number of cracks were fewer than in the lower boron vacuum-induction heat V-15 (fig. 2(a)) but the cracks appeared to be deeper.

The oxygen, nitrogen, and phosphorous in the arc heat compared to the induction heat, as follows:

<u>Melting variable</u>	<u>N, (weight, percent)</u>	<u>O, (weight, percent)</u>	<u>P, (weight, percent)</u>
Vacuum- induction	<0.001 to 0.002	0.0013 to 0.0037	0.004 to 0.008
Vacuum-arc	0.004	0.0022	0.011

The analyses indicate that these elements were brought down to nearly the same level during vacuum-arc melting as during vacuum-induction melting.

#### Air-Induction Melting

Heats melted in air were more prone to corner cracking during hot-rolling than vacuum heats at comparable boron and zirconium contents (compare heat A-6, fig. 2(e) with heat V-12, fig. 2(b); also heat A-3, fig. 2(f) with heat V-25, fig. 2(c)). The heats melted in air were also subject to "peeling" of the surface in all stages of the reduction from the ingot to bar stock. It should be recognized that boron did reduce corner cracking in heats melted in air but it was not as effective as in vacuum heats.

The creep-rupture properties of heats melted in air with low zirconium (figs. 3, 4, and 5) were more a function of boron content than of variations in melting practice. Rupture times and creep resistance were perhaps slightly lower for the heats melted in air with low boron contents. There was, however, little difference for heat A-6 with 0.0058 percent boron. The duplicate tests (table IV), however, for heat A-6 did show more variation than for the vacuum heats. Increasing the zirconium content of low boron heats melted in air to 0.07 percent did not bring the rupture time (fig. 6) up to that of heats melted in vacuum with the same zirconium content. Ductilities also averaged lower (fig. 7) and were erratic. Air heats with low boron and zirconium had

lower properties than comparable vacuum heats. For this reason the degree of improvement from zirconium appeared to be similar for both types of melting.

Adding 0.08 to 0.10 percent of zirconium in the presence of substantial amounts of boron (heats A-3 and A-4) resulted in longer rupture times (fig. 8) for heats melted in air than for heats melted in vacuum. Ductilities were comparable (fig. 8). Air melting may have prevented some of the falloff in properties encountered in vacuum heats resulting from increased zirconium with high boron. Although two air heats (A-3 and A-4) did have high Ti plus Al contents, it is estimated that this difference alone did not account for the increase in rupture times.

These results from a limited number of heats indicated that boron and/or zirconium had far more influence on creep-rupture properties at 1,600° F than the melting method. Air melting, however, had the following minor adverse effects in comparison to vacuum melting for a given boron and zirconium content:

(a) Slightly lower rupture strengths and ductilities. The only exception was high zirconium and boron where air melting apparently reduced the loss in strength resulting from more than optimum amounts of boron plus zirconium.

(b) More tendency to crack during hot-working with a poor surface due to peeling.

Vacuum melting did result in lower nitrogen, oxygen, and phosphorous than did air melting as is shown by the following comparison:

<u>Melting conditions</u>	<u>N, (weight, percent)</u>	<u>O, (weight, percent)</u>	<u>P, (weight, percent)</u>
Vacuum	<0.001 to 0.002	0.0013 to 0.0037	0.004 to 0.008
Air	0.010 to 0.048	0.0012 to 0.0179	0.009 to 0.025

Accordingly, additional experiments were undertaken in which the influence of these elements were studied.

#### Influence of Nitrogen, Oxygen, and Phosphorous

The influence of nitrogen, oxygen, and phosphorous was studied by melting in vacuum and then adding these elements. This part of the research was restricted to heats in which boron was added in the absence of zirconium.

Vacuum-induction plus argon melting: Heats were melted in vacuum and then argon was admitted to the chamber in order to be able to add nitrogen and oxygen and retain them in the heat. Heats V + Arg-3, V + Arg-7, and V + Arg-10 were melted this way without any subsequent additions as control heats to check any effects from the change in melting procedure. The oxygen, nitrogen, and phosphorous contents were similar to vacuum-melted heats.

Recovery of nitrogen and oxygen was erratic even when these elements were added in the presence of argon. Analyses showed that V + Arg-5, V + Arg-6, V + Arg-8, and V + Arg-11 showed no significant differences in these elements in comparison to the control heats or to vacuum heats. Accordingly, these heats were used as further control heats to check the reliability of the analyses in predicting properties.

The rupture and creep properties of the heats exposed to argon after vacuum melting were similar to those of vacuum heats with equivalent boron (figs. 3, 4, and 5). It, therefore, appeared that argon did not influence properties and the curves of figures 3, 4, and 5 were actually based on the data for the V + Arg heats as well as vacuum heats. The properties were in accordance with those which would be expected from the results of the analyses for nitrogen, oxygen, and phosphorous. The following comparison shows that there was only a slight difference in these elements.

<u>Melting variable</u>	<u>N, (weight, percent)</u>	<u>O, (weight, percent)</u>	<u>P, (weight, percent)</u>
Vacuum	<0.001 to 0.002	0.0013 to 0.0037	0.004 to 0.008
Vacuum + Argon	0.003 to 0.006	0.0015 to 0.0027	<0.005 to 0.011
Vacuum + Argon with nitrogen or oxygen additions without recovery	0.004	0.0008 to 0.0029	0.005 to 0.010

Effect of nitrogen: Sufficient nitrogen was recovered in heats V + Arg-1 (N), V + Arg-9 (N), and V + Arg-12 (N) to cover the range for nitrogen in heats melted in air. The analyzed values for nitrogen, oxygen, and phosphorous are compared in the following tabulation with the values for V + Arg heats and for heats melted in air:

<u>Heats</u>	<u>N, (weight, percent)</u>	<u>O, (weight, percent)</u>	<u>P, (weight, percent)</u>
All V + Arg heats	0.003 to 0.006	0.0008 to 0.0029	<0.005 to 0.011
V + Arg-1 (N)	0.010	0.0013	0.007
V + Arg-9 (N)	0.048	0.0051	0.013
V + Arg-12 (N)	0.041	0.0035	0.006
Air melted	0.010 to 0.048	0.0012 to 0.0179	0.009 to 0.025

For unknown reasons the oxygen in heat V + Arg-9 (N) was high.

Reference to table IV and figure 3 shows that these compositional variations had no effect on rupture time, except possibly a slight reduction of rupture time of heat V + Arg-1 (N). The ductility of heat V + Arg-9 (N) was high (fig. 4). This heat as well as heat V + Arg-1 (N) also had slightly higher minimum creep rates (fig. 5).

The results of these few heats indicate that increased nitrogen had very little effect in heats with about 0.005 percent boron. The high ductility of heat V + Arg-9 (N) may be related to the high combined oxygen plus nitrogen content as is discussed later.

Effect of oxygen: One heat (V + Arg-4 (O)) was made with the oxygen increased after vacuum melting. The comparative values for oxygen, nitrogen, and phosphorous were as follows:

<u>Heats</u>	<u>O, (weight, percent)</u>	<u>N, (weight, percent)</u>	<u>P, (weight, percent)</u>
All V + Arg heats	0.0008 to 0.0029	0.003 to 0.006	<0.005 to 0.011
V + Arg-4 (O)	0.0080	0.005	<0.005
Air melts	0.0012 to 0.0179	0.010 to 0.048	0.009 to 0.025

The oxygen had no effect on rupture time (fig. 3) and probably none on ductility (fig. 4) or creep resistance (fig. 5). The properties are within the scatter to be expected at a boron level of 0.0078 percent.

Vacuum plus air melting: One heat (V + air) was exposed to air after melting in vacuum to determine if there would be any difference from straight air melting. The analyzed variations in the elements influenced by vacuum melting were as follows:

<u>Melting variable</u>	<u>N, (weight, percent)</u>	<u>O, (weight, percent)</u>	<u>P, (weight, percent)</u>
Vacuum	<0.001 to 0.002	0.0013 to 0.0037	0.004 to 0.008
Vacuum + air	0.055	0.0084	<0.005
Air	0.010 to 0.048	0.0012 to 0.0179	0.009 to 0.025

The 15 minutes of exposure to air resulted in nitrogen and oxygen levels similar to air-melted heats with low phosphorous.

The exposure to air after vacuum melting increased the tendency for corner cracking during hot-rolling over vacuum melting. There was, however, no surface peeling (compare fig. 2(g) with fig. 2(b)).

The rupture times (fig. 3) and creep resistance (fig. 5) were possibly slightly low for the boron content. Ductility was, however, high (fig. 4).



These results from one heat suggest that oxygen plus nitrogen increase ductility after vacuum melting. It was previously shown that heat V + Arg-9 (N) with high oxygen plus nitrogen also had high ductility. If the indicated improvement in ductility in rupture tests at 1,600° F for oxygen plus nitrogen is true, vacuum melting must remove some unidentified element which is deleterious to ductility. When present simultaneously oxygen and nitrogen are probably beneficial to ductility and their removal by vacuum melting actually reduces ductility. Oxygen plus nitrogen, however, does appear to increase corner cracking during hot-rolling.

Effect of phosphorous: One heat (V + Arg-2 (P)) was vacuum melted and then phosphorous was added to bring the level up to that of air heats. This heat with 0.024 percent phosphorous had the same properties (figs. 3, 4, and 5) as vacuum-melted heats with less than 0.008 percent phosphorous at a boron level of about 0.0050 percent.

This one heat indicates that the removal of phosphorous during vacuum melting probably had little effect on creep-rupture properties at 1,600° F.

#### Elements Volatilized by Vacuum Melting

In view of the finding that vacuum melting may be removing elements detrimental to ductility and that oxygen plus nitrogen in the amounts characteristic of air melting may be actually beneficial to ductility, a simple experiment designed to obtain qualitative information on the elements volatilized during vacuum melting was carried out. A cold nickel plate was suspended over a melt for 20 minutes and semiquantitative spectrographic analyses were made for elements condensed on the plate. The results (table III) indicated the Cr, Co, Ni, and Mo were present in amounts roughly proportional to the amounts in the alloy and their relative volatilities. Mn, Al, and Si were also present as expected. The B, Ca, and Mg would be expected to be beneficial to ductility. The effect of copper is not known. The presence of phosphorous was not unexpected because analyses showed that it was removed during vacuum melting. It has been shown in the previous section, however, that it did not affect ductility.

The elements detected which seem most likely to account for improved ductility as a result of vacuum melting are lead and/or silver. Lead is reportedly detrimental in the type of alloy studied in amounts as low as 1 to 10 parts per million. The comparative chemical analyses (table IV) for air- and vacuum-melted heats were not sufficiently sensitive to differentiate in the lead and silver contents of the two types of heats.

It is to be emphasized that this study was by no means complete or conclusive. A far more thorough study would be required to be conclusive.

#### Effects of Melting Practices on Microstructures

In reference 1 it was shown that boron and zirconium in vacuum-induction heats improved creep-rupture properties by retarding the microcracking in the grain boundaries which led to fracture. When boron and zirconium were very low,  $M_{23}C_6$  type compounds rapidly agglomerated at the grain boundaries along with  $\gamma'$ , the  $Ni_3(Al,Ti)$  precipitate in the alloy. When stress was present, the matrix adjacent to grain boundaries transverse to the applied stress became depleted of  $\gamma'$  particles. Microcracks formed between the  $M_{23}C_6$  precipitates and the depleted matrix, grew and linked together to cause early fracture with low ductility. This process was retarded by zirconium and especially by boron. In heats containing boron the initial carbide precipitates formed within the grains apparently as  $M_6C$  type compounds, and  $\gamma'$  depletion adjacent to the transverse grain boundaries was retarded. As a result the first appearance of microcracks changed from early in primary creep in the absence of boron or zirconium to third-stage creep when 80 to 90 parts per million of boron was present. No evidence of an effect from boron or zirconium on the  $\gamma'$  distribution or stability was found. Other structural differences studied were either unaffected or did not appear to be related to properties.

In order to obtain information on the effect of oxygen, nitrogen, and air melting on these structural characteristics, selected heats from the present investigation were subjected to similar microstructural examination. These data were then compared to values measured on typical vacuum-induction heats (table V). The role of  $M_{23}C_6$  carbides in microcracking was found to be similar to that in reference 1. Accordingly the discussion of the structural effects from the melting conditions discussed in the following sections is restricted to the changes arising from the melting variables.

In carrying out the microstructural examinations, the main effort was placed on specimens which had been exposed to aging during the accumulation of 2 percent creep in about 240 hours. This provided a series of specimens which had been exposed for an equal time and to equal strain at 1,600° F for evaluation of structural differences. Heats V + Arg-4 (O), V + Arg-7, V + Arg-9 (N), V + air, and A-6 were exposed at 25,000 psi. V + Arg-1 (N) was exposed under 23,000 psi. These were the conditions of exposure for the data in table V.

Structural effects of air melting: Hardness values as a function of aging time at 1,200°, 1,400°, and 1,600° F were used as a possible measure of the effect of air melting on the  $\gamma'$  reaction. Comparative values for a vacuum heat (V-12) and an air heat (A-6) are shown in figure 9. The vacuum heat was slightly harder when aged for 1 hour at 1,400° and 1,600° F with no significant difference for the longer time periods. The vacuum heat did not become harder until nearly 100 hours of aging at 1,200° F. Such differences in hardness as were present could be due to the boron difference (0.0058 percent in A-6 and 0.0089 percent in V-12) as well as to the differences in melting conditions.

The surface density of  $\gamma'$  particles in heat A-6 after aging at 1,600° F was the same as for heat V-12. This is shown by figure 10. Actual counts gave the same value for heat A-6 as was obtained in reference 1 for heat V-12. This finding together with the hardness measurements indicates that there was very little effect on the  $\gamma'$  reaction from air melting.

Figure 11 shows microstructures after 2-percent creep deformation. The number of microcracks in a specimen of heat A-6 was more than double (table V) the number in heat V + Arg-7. This comparison was used because the boron levels were similar in these two heats. The number of grain boundaries with  $\gamma'$  depletion in the adjacent matrix was, however, considerably less in the air heat. The air heat had a slightly smaller grain size.

The most significant microstructural feature found in heat A-6 was the tendency for microcracks to occur at titanium carbonitride particles present in the grain boundaries. The electron micrograph of heat A-6 in figure 10(b) shows a crack at a Ti(C,N) particle. Some of the cracks shown in the X1000 optical photomicrograph (fig. 11(e)) also occurred at Ti(C,N) particles. It seemed evident that the increased microcracking of heats melted in air was due to Ti(C,N) particles that happened to be in grain boundaries. As figure 11(e) shows, there were many particles within the grains, which tended to be in stringers in the direction of rolling. Microscopic examination indicated that these particles were primarily Ti(C,N) which appeared orange in color indicating a high percentage of nitrogen.

In vacuum heats or vacuum plus argon heats, the number of Ti(C,N) particles in the stringers was considerably less than in heat A-6 (compare fig. 11(a) with 11(e)). No evidence was found to indicate that microcracking was initiated by Ti(C,N) particles in vacuum heats. Most of these Ti(C,N) particles were gray in color indicating that the particles were carbon rich.

The lower incidence of  $\gamma'$  depletion in the air heat is not understood. Previous consideration of the subject suggested that  $\gamma'$  depletion was closely connected with microcracking. These limited results suggest that either it is less important than was believed or the initiation of microcracks by  $\text{Ti}(\text{C},\text{N})$  particles in air melting offsets the effect of reduced  $\gamma'$  depletion.

Structures of heats with nitrogen and oxygen added after vacuum melting: Adding nitrogen after vacuum melting (heat V + Arg-1 (N) with 0.010 percent nitrogen) resulted in a slight reduction in the amount of microcracking (table V) after 2 percent creep in comparison to a vacuum heat (V + Arg-7) with the same boron content. The number of depleted grain boundaries may have been slightly increased. Grain sizes were similar. Microstructures are not shown for heat V + Arg-1 (N). In examining the heat it was noted that the number of  $\text{Ti}(\text{C},\text{N})$  particles was increased. They were not, however, associated with microcracking.

Heat V + Arg-9 (N) with 0.048 percent nitrogen and 0.0051 percent oxygen microcracked (table V) about the same amount as heat V + Arg-7 which had low nitrogen and oxygen. The number of grain boundaries depleted of  $\gamma'$  was slightly reduced. Grain sizes were similar. The creep-rupture properties of this heat were similar to those of heat V + Arg-7 except that the ductility was abnormally high. The microcracks and  $\gamma'$  depletion data do not account for the high ductility. The number of  $\text{Ti}(\text{C},\text{N})$  particles (fig. 11(c)) was increased by the nitrogen addition and they formed stringers similar to those of heat V + air. The color of these particles indicated an increase in the proportion of nitrogen to carbon. The  $\text{Ti}(\text{C},\text{N})$  particles in the grain boundaries did not initiate microcracks. The number of oxide particles, mainly  $\text{Al}_2\text{O}_3$ , was also higher in comparison to vacuum melting in accordance with the high oxygen content.

Adding oxygen after vacuum melting (heat V + Arg-4 (O)) resulted in some increase in microcracking (table V) and grain boundaries depleted of  $\gamma'$ . This could be the reason for the slightly reduced rupture life and ductility. The high oxygen resulted in an increase in the number of oxide particles present in the stringers in comparison to vacuum melting (fig. 11(b)). The oxide particles were not associated with microcracks. Figure 11(b) shows one microcrack in a grain boundary which appeared to be initiated by a carbide particle.

The exposure to air after vacuum melting (heat V + air) resulted in a pronounced increase in the number of  $\text{Ti}(\text{C},\text{N})$  and  $\text{Al}_2\text{O}_3$  particles counted in the structure represented by figure 11(d). The  $\text{Ti}(\text{C},\text{N})$  particles were orange in color indicating a high proportion of nitrogen. There was no evidence of microcracking associated with these particles. In fact, the number of microcracks (table V) was substantially lower

and the number of depleted grain boundaries slightly lower than for vacuum heat V-12 after 2 percent creep. This apparently accounts for the abnormally high ductility of this material in the rupture tests.

General aspects of structural studies: The  $\gamma'$  density count for the heats examined did not show a significant difference after 2 percent creep. No evidence was found to indicate that any of the observed effects were due to alteration of the  $\gamma'$  reaction.

The outstanding finding was the initiation of microcracks by Ti(C,N) particles in the grain boundaries of the heat melted in air and the absence of this after vacuum melting even when nitrogen and oxygen were built up to equal or higher levels. If heat V + Arg-9 (N) with both high nitrogen and oxygen had also shown reduced microcracking, it would appear quite definite that the simultaneous presence of nitrogen and oxygen in amounts characteristic of air melting increased ductility by reducing microcracking. However, heat V + Arg-9 (N) did not show a pronounced reduction in microcracking even though it did have high ductility.

All of the samples were examined for other microstructural characteristics such as carbides and mixed nodules of  $\gamma'$  and carbide within the grains without finding any difference among the heats.

## DISCUSSION

The most striking result was the demonstration that boron and zirconium content of the alloy studied was more influential on creep-rupture properties at 1,600° F than broad melting practice variations. The properties of heats melted by induction in air or vacuum or by the vacuum-arc process were at most only slightly different at equal levels of boron and/or zirconium. This is illustrated by figure 12 which shows approximate stress-rupture time curves drawn from the data of reference 1 to show the ranges in properties of vacuum-induction heats from the variations in boron and/or zirconium. Rupture times for heats air or vacuum-arc melted are compared to the stress-rupture time curves for vacuum-induction heats with equivalent boron and zirconium contents to illustrate the much larger effect of those elements than the melting method.

The limited results obtained indicated that vacuum melting did show certain advantages in comparison to melting in air:

1. Creep-rupture properties were somewhat better at low levels of boron and zirconium or at high levels of zirconium. However, at high boron levels there was little difference, and in the presence of high levels of boron plus zirconium air melting gave the highest strengths.

2. The duplicate rupture tests were more consistent for vacuum-melted than for air-melted heats.

3. Corner cracking during hot-rolling was reduced and poor surface from peeling was eliminated by vacuum melting.

4. Heats melted in vacuum generally had fewer titanium carbonitrides and oxides. There was, however, considerable variation in this respect in air heats suggesting that for air melting, cleanliness is to some degree a function of the opportunity for oxides and nitrides to separate from the melt. The difficulty encountered in recovering oxygen or nitrogen added after vacuum melting support this aspect of the results. The generally larger number of inclusions in air heats would be expected to have more detrimental effects on transverse properties than were found from the tests on longitudinal specimens. Also they would be expected to be detrimental to other properties.

While the experiments were limited, they seemed to indicate that nitrogen plus oxygen contents characteristic of air melting were actually beneficial to ductility in the rupture tests. If so, this suggests that vacuum melting removed unidentified elements which were detrimental to ductility. There seems to be little doubt that there was an effect of this type. There is some doubt, however, that the case was very well proved that nitrogen plus oxygen was required after vacuum melting to obtain a marked improvement in ductility. All heats to which oxygen or nitrogen were added after vacuum melting gave erratic creep-rupture test results. It may be that the two heats with high nitrogen plus oxygen (heats V + Arg-9 (N) and V + air) accidentally happened to give duplicate test results with high ductility.

Oxygen and nitrogen appeared to be responsible for an increased tendency to corner crack during hot-rolling. They did not, however, appear to be the cause of poor surface due to peeling in air heats. Apparently, vacuum melting removed elements responsible for this effect, and the peeling was not related to the oxide-carbonitride stringers.

The evidence seemed quite conclusive that  $Ti(C,N)$  particles in grain boundaries initiated microcracking in heats melted in air. However, these particles were not responsible alone for this effect since their tendency to initiate cracks was removed by prior vacuum melting. Apparently, some unidentified elements removed by vacuum melting were required to cause  $Ti(C,N)$  particles to initiate microcracks.

The relation of microcracking at  $M_{23}C_6$  particles to creep-rupture properties was obscured by the data. Heat V + Arg-9 (N) had high ductility apparently as a result of high nitrogen plus oxygen after vacuum melting. It, however, showed little change in microcracking in

comparison to vacuum heats while heat V + air showed a marked reduction in microcracking. It would seem that some other factor was involved. Possibly the higher boron in heat V + air was a factor. At least relative microcracking tendencies alone did not seem to explain the increased ductilities from oxygen plus nitrogen.

The data suggest that the increased microcracking from Ti(C,N) particles in air heats at low levels of boron and zirconium combined with the high sensitivity to microcracking at  $M_{23}C_6$  particles was responsible for reduced properties. This effect was, however, lost at high levels of boron. Possibly the improvement in ductility due to the presence of oxygen plus nitrogen offset the increased microcracking from Ti(C,N) particles.

The significance of analyses for nitrogen and oxygen is open to question. The results indicated that the amounts were a function of the number of oxide and Ti(C,N) particles present. These in turn were a function of the opportunity for them to separate from the melt. The microstructural studies indicated that these particles had little effect on properties after vacuum melting. This suggests then that they were related to the amount of oxygen and nitrogen in solution and that this was the main factor in the effects on properties.

The reliability of the analyses for oxygen and nitrogen is also open to question. The results obtained appeared to be consistent between heats. There is, however, doubt that the values obtained were quantitatively correct since the analytical procedures are questionable. Furthermore, segregation of oxides and nitrides could have influenced results.

The structural studies were incomplete in that only heats with substantial amounts of boron were studied. More confidence in the results would have been possible if the melting practice effects on structure had been studied for a wider range in boron and/or zirconium. The studies involving variation in nitrogen and oxygen after vacuum melting were also limited to heats with considerable boron present. The number of heats was also too limited for confidence. While study of the effect of oxygen and nitrogen was interesting, the relatively minor effects in comparison to boron and zirconium reduced the incentive to do extensive research on these effects.

There were variations in the major alloying elements in the heats. These could not be related to property variations with the exception of a few cases of high Ti plus Al and possibly high ductility from high carbon.

Care should be exercised in extending the results to other alloys without more experimental evidence. It is believed, however, that the

results will be fairly general for nickel base alloys strengthened with Ti plus Al.

### CONCLUSIONS

A limited study of the influence of vacuum-induction, air-induction, and cold-mold vacuum-arc melting for a 55Ni-20Cr-15Co-4Mo-3Ti-3Al alloy permits the following conclusions:

1. The boron and/or zirconium contents of the alloys had far more influence on creep-rupture properties at 1,600° F than the melting methods.

2. Vacuum melting, however, had the following advantages:

(a) Considerably less susceptibility to corner cracking and a better surface during hot-rolling.

(b) More uniform creep-rupture properties within a given heat.

(c) Slightly better creep-rupture properties in heats with low boron plus zirconium and in heats with zirconium. There was no advantage at high boron levels, and air heats were superior at high levels of boron plus zirconium.

(d) The vacuum heats had fewer oxide and titanium carbonitride inclusions. This difference, however, appeared to be a function of the opportunity for the inclusions to separate from the melt in heats high in oxygen plus nitrogen.

3. A limited study of the role of oxygen and nitrogen indicated that these elements were beneficial to ductility in creep-rupture tests. The data suggest that vacuum melting removes unidentified elements which are detrimental to ductility.

4. Oxygen and nitrogen increase corner cracking during hot-rolling. They are not, however, responsible for the poor surface from peeling during rolling of air heats, nor was the increase in oxides and carbonitrides.

5. Titanium carbonitrides in the grain boundaries initiate microcracking in air-melted heats but not in heats first melted in vacuum. Oxides did not initiate microcracks. The relation of microcracking as influenced by oxygen and nitrogen to creep-rupture properties was not clear from the data.



6. The reduction of phosphorous by vacuum melting was not related to properties.

University of Michigan,  
Ann Arbor, Mich., September 10, 1958.

#### REFERENCES

1. Decker, R. F., Rowe, J. P., and Freeman, J. W.: Boron and Zirconium From Crucible Refractories in a Complex Heat-Resistant Alloy. NACA Rep. 1392, 1958. (Supersedes NACA TN 4049 and NACA TN 4286.)
2. Wilkins, D. H., and Fleischer, J. F.: The Determination of Oxygen in Titanium Vacuum Fusion with a Platinum Bath. *Analytica Chim. Acta*, vol. 15, no. 4, Oct. 1956, pp. 334-336.
3. Hague, J. L., Paulson, R. A., and Bright, H. A.: Determination of Nitrogen in Steel. Res. Paper 2021, Jour. Res., Nat. Bur. Standards, vol. 43, no. 3, Sept. 1949, pp. 201-207.
4. Bigelow, W. C., Amy, J. A., and Brockway, L. O.: Electron Microscopic Identification of the  $\gamma'$  Phase of Nickel-Base Alloys, *Proc. ASTM*, vol. 56, 1956, pp. 945-953.

TABLE I.- CHEMICAL ANALYSES OF EXPERIMENTAL HEATS

[Balance is nickel]

Heat	Runs	Vacuum fusion		Elements present, weight percent										
		O	N	B	Zr	C	Ti	Al	Cr	Co	Mo	Si	Mn	P
V-11	1	0.0021	0.001	0.0017	<0.01	0.05	3.25	3.58	20.0	16.2	4.20	0.18	0.10	0.004
V-12	1	.0017	.001	.0089	<.01	.10	3.15	3.25	20.9	14.8	4.20	.20	<.10	.004
V-13	1	.0020	.002	.0003	<.01	.05	3.25	3.37	20.4	14.8	4.20	.25	.12	.007
V-15	1	.0013	.001	.0002	<.01	.08	3.08	3.35	19.7	15.0	3.90	.17	.13	.006
V-17	1	.0023	.001	.0074	<.01	.07	3.02	3.26	19.4	16.5	3.75	.16	.12	.008
V-20	1	.0022	.001	.0010	<.01	.12	2.92	3.45	20.3	15.2	4.05	.15	.10	.007
V-21	1	.0015	<.001	.0004	<.01	.15	2.85	3.42	20.2	16.1	3.95	.15	.10	.007
V-25	1	.0037	.002	.0060	.06	.10	3.24	2.94	19.4	15.9	4.10	.16	<.10	.007
V-Arc	1	.0022	.004	.0006	.015	.12	3.15	3.05	18.6	16.3	4.00	.09	.15	.011
V + Arg-1(N)	2	.0013	.010	.0046	<.01	.20	2.76	3.42	20.5	15.7	3.95	.20	<.10	.007
V + Arg-2(P)	1	.0017	.003	.0055	<.01	.17	2.87	3.49	21.5	15.1	4.10	.20	.10	.024
V + Arg-3	2	.0027	.006	.0094	<.01	.16	3.08	3.50	20.7	15.8	4.25	.18	<.10	<.005
V + Arg-4(O)	2	.0080	.005	.0078	<.01	.17	3.08	3.12	20.2	15.4	4.15	.14	<.10	<.005
V + Arg-5	3	.0010	.004	.0100	<.01	.13	2.88	3.20	20.0	14.8	4.05	.13	<.10	<.005
V + Arg-6	2	.0012	.004	.0097	<.01	.16	2.85	3.11	20.0	15.3	4.20	.15	<.10	<.005
V + Arg-7	2	.0015	.004	.0057	<.01	.12	3.20	3.11	18.8	15.8	3.80	.32	<.10	.011
V + Arg-8	2	.0008	.004	.0046	<.01	.12	3.18	3.20	19.0	15.8	3.80	.28	<.10	.010
V + Arg-9(N)	2	.0051	.048	.0055	<.01	.12	3.35	3.20	18.8	15.8	3.80	.23	<.10	.013
V + Arg-10	2	.0025	.003	.0038	<.01	.13	3.15	3.30	20.0	14.8	4.20	<.20	<.10	.007
V + Arg-11	2	.0029	.004	.0054	<.01	.14	3.24	3.51	20.6	15.0	4.25	<.20	<.10	.006
V + Arg-12(N)	2	.0035	.041	.0057	<.01	.15	3.24	3.48	19.6	15.1	4.25	<.20	<.10	.006
V + Air	3	.0084	.055	.0090	<.01	.17	2.97	3.15	19.9	15.2	4.10	.16	<.10	<.005
A-1	3	.0179	.026	none added	<.01	.13	3.15	3.36	20.0	16.7	3.90	.10	<.10	-----
A-2	3	.0088	.026	.0004	<.01	.09	3.55	3.27	20.2	15.6	3.85	.14	<.10	.012
A-3	2	.0043	.030	.0096	.08	.10	3.48	3.26	19.2	15.7	3.90	.15	.20	.025
A-4	2	.0048	.048	.0069	.10	.10	3.50	3.45	19.8	14.7	4.15	.15	.18	.020
A-5	2	.0012	.010	.0003	.07	.15	2.82	3.30	20.5	16.4	3.90	.14	.12	.009
A-6	2	.0050	.028	.0058	<.01	.13	2.94	3.35	20.2	15.6	3.95	.17	.11	.010

Mg in all heats &lt;.01

Fe in all heats &lt;.30

Cu in all heats &lt;.10

TABLE II.- CHEMICAL ANALYSES OF SELECTED HEATS  
FOR TRACE ELEMENTS

Heat	Composition, weight percent					
	Mg		Ca	Pb		S
	Lab 1	Lab 2		Lab 1	Lab 2	
<sup>a</sup> V-13	(b)	<.001	(b)	(b)	(b)	(b)
V-15	(b)	(b)	(b)	(b)	(b)	.007
<sup>a</sup> V-20	.001	<.001	.001	<.001	.004	(b)
<sup>a</sup> V-21	(b)	<.001	(b)	(b)	.002	(b)
A-2	(b)	(b)	(b)	(b)	(b)	.008
<sup>a</sup> A-5	(b)	(b)	(b)	(b)	.002	(b)
A-6	.001	(b)	.001	<.001	(b)	(b)

<sup>a</sup>Ba, Be, Bi, Ag, Na, Sn, V, Zn not detected.

<sup>b</sup>No analysis was made.

TABLE III.- SEMIQUANTITATIVE SPECTROGRAPHIC ANALYSIS  
OF CONDENSATE FROM VACUUM MELT

[Condensate collected on cold nickel plate held over melt  
20 minutes at 2,700° F under 5 microns pressure.]

Weight percent of indicated element in condensate					
>10	1 - 10	0.1-1	0.01 - .1	0.001 - .01	<0.001
Cr Co Mn	Ni	P	Al Cu Pb	B Ca Mg Mo Si	Ag

TABLE IV.- CREEP-RUPTURE DATA AT 1600° F AND 25,000 PSI

Heat	Additions	Compositional variables, weight percent					Rupture			
		O	N	B	Zr	P	Life, hr	Elongation, percent	Reduction of area, percent	Minimum second- stage creep rate, percent/hr
Vacuum-induction melted										
V-11	<sup>a</sup> none	0.0021	0.001	0.0017	<0.01	0.004	185 230	3 5	2 5	0.0030 .0029
V-12	0.01B	.0017	.001	.0089	<.01	.004	429 394	10 7	11 8	.0018 -----
V-13	none	.0020	.002	.0003	<.01	.007	57 48	2 1	2 1	.0040 -----
V-15	none	.0013	.001	.0002	<.01	.006	45 52	2 2	1 1	.0160 .0060
V-17	.01B	.0023	.001	.0074	<.01	.008	400 346	7 7	6 5	.0013 -----
V-20	<sup>a</sup> none	.0022	.001	.0010	<.01	.007	225 207	5 4	4 3	.0025 .0034
V-21	<sup>a</sup> none	.0015	<.001	.0004	<.01	.007	103 106	4 3	2 2	.0066 .0064
V-25	.10Zr +.01B	.0037	.002	.0060	.06	.007	314 474 444 360	6 7 8 7	6 10 12 7	.0019 .0011 ----- .0007
Vacuum-arc melted in cold mold										
V-Arc	none	.0022	.004	.0006 .0005	.015	.011	76 58 72 89	4 5 5 7	3 7 6 7	.0165 .0180 .0215 .0170
Vacuum + argon - induction melted										
V + Arg-1(N)	.01B+ .03N	.0013	.010	.0046	<.01	.007	205 188 185 186	5 3 7 12	5 3 7 12	.0065 .0050 .0077 .0066
V + Arg-2(P)	.01B+ .025P	.0017	.003	.0055	<.01	.024	266 284	5 8	6 8	.0038 .0048
V + Arg-3	.01B	.0027	.006	.0094	<.01	<.005	546 585	10 14	12 16	.0014 .0008
V + Arg-4(O)	.01B+ .0030	.0080	.005	.0078	<.01	<.005	278 373 294 274	3 6 14 (interrupted at 2.0)	7 6 15 --	.0030 .0030 .0040 .0040
V + Arg-5	.01B+ .0060	.0010	.004	.0100	<.01	<.005	470 329 300	6 11 12	6 14 13	.0018 .0032 .0030

<sup>a</sup> B pickup from magnesia crucibles.

TABLE IV.- CREEP-RUPTURE DATA AT 1600° F AND 25,000 PSI - Concluded

Heat	Additions	Compositional variables, weight percent					Rupture			
		O	N	B	Zr	P	Life, hr	Elongation, percent	Reduction of area, percent	Minimum second- stage creep rate, percent/hr
Vacuum + argon - induction melted										
V + Arg-6	.01B+ .09N	0.0012	0.004	0.0097	<0.01	<0.005	386 338	12 6	14 7	0.0025 .0024
V + Arg-7	.005B	.0015	.004	.0057	<.01	.011	306 290 373 244	7 6 9 (interrupted at 2.0)	11 10 10 --	.0047 .0031 .0025 .0025
V + Arg-8	.005B +.006 O	.0008	.004	.0046	<.01	.010	313 305 290 276	6 5 6 6	8 6 8 7	.0016 .0028 .0026 .0028
V + Arg-9(N)	.005B +.09N	.0051	.048	.0055	<.01	.013	288 232 256 242	12 15 14 (interrupted at 2.0)	14 19 19 --	.0030 .0063 .0090 .0037
V + Arg-10	.005B	.0025	.003	.0038	<.01	.007	270 226	7 6	6 7	.0032 .0034
V + Arg-11	.005B +.006 O	.0029	.004	.0054	<.01	.006	350 414	6 9	6 8	.0016 .0013
V + Arg-12(N)	.005B +.09N	.0035	.041	.0057	<.01	.006	420 343	12 11	9 12	.0022 .0015
Vacuum + air - induction melted										
V + Air	.01B	.0084	.055	.0090	<.01	<.005	251 295 341 244	16 16 9 (interrupted at 2.0)	16 22 13 --	.0042 .0051 ----- .0038
Air induction melted										
A-1	none	.0179	.026	-----	<.01	-----	24 22	4 1	<1 1	.0180 -----
A-2	none	.0088	.026	.0004	<.01	.012	20 27	2 1	<1 1	----- .0116
A-3	.01B+ .10Zr	.0043	.030	.0096	.08	.025	436 416	6 9	8 11	.0015 .0020
A-4	.01B+ .10Zr	.0048	.048	.0069	.10	.020	448 471	8 9	8 9	.0020 .0006
A-5	.10Zr	.0012	.010	.0003	.07	.009	22 43 41 47	1 2 4 4	2 1 5 5	----- .0025 .0320 .0430
A-6	.01B	.0050	.028	.0058	<.01	.010	155 273 254 271 290 226	4 3 8 10 9 (interrupted at 2.0)	3 3 8 10 9 --	.0022 .0015 .0035 .0021 .0025 .0037

TABLE V.- MICROSTRUCTURAL FEATURES OF HEATS

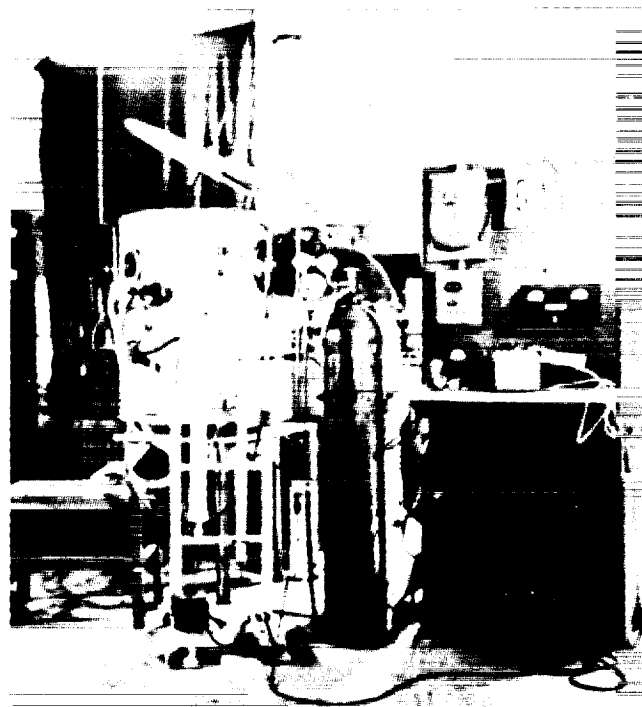
[After 2 percent creep deformation at 1,600° F in 240 hours]

Heat	Microcracks (b)	Depleted grain boundaries (c)	ASTM grain size
0.0078 to 0.0090 percent Boron			
<sup>a</sup> V-12	50	75	3
V + Arg-4(O)	81	111	3
V + Air	19	69	3
0.0046 to 0.0058 percent Boron			
V + Arg-7	76	155	3
V + Arg-1(N)	56	177	3
V + Arg-9(N)	65	134	3
A-6	199	95	4

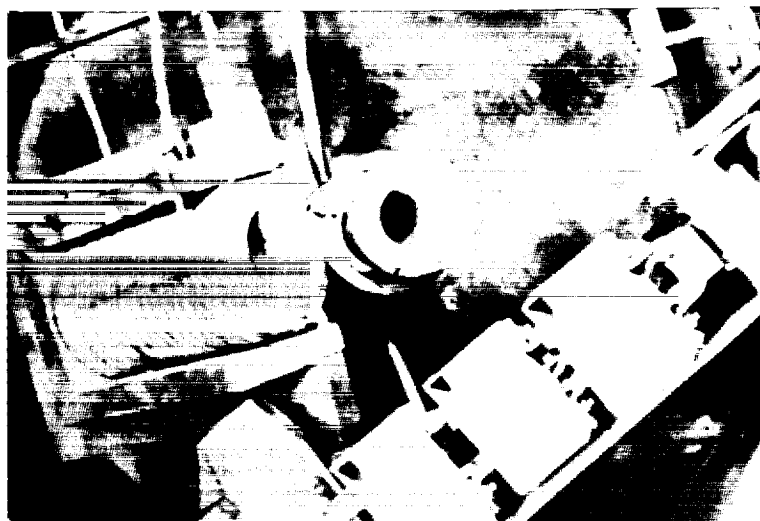
<sup>a</sup>Number of microcracks and depleted grain boundaries interpolated for 2 percent creep from reference 1.

<sup>b</sup>Microcracks detected at X1000, in 0.008 sq in.

<sup>c</sup>Grain boundaries where depletion was detected at X1000, in 0.008 sq in.



(a) External view.



(b) Internal view of crucible, charge buckets and ingot mold.


L-59-1934

Figure 1.- University of Michigan vacuum-melting furnace.



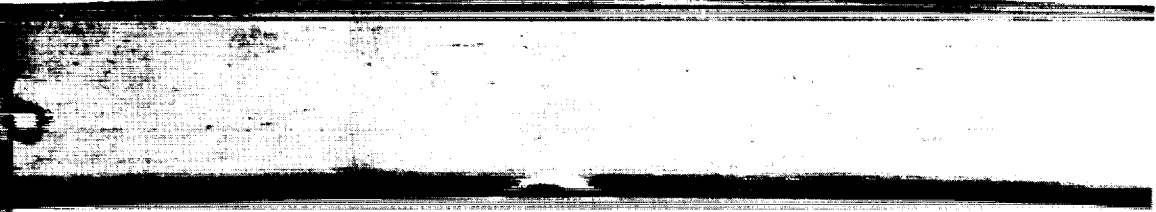
1148

- (a) Heat V-15, vacuum-induction melted with 0.0002 percent B, less than 0.01 percent Zr, 0.0013 percent O, and 0.001 percent N.

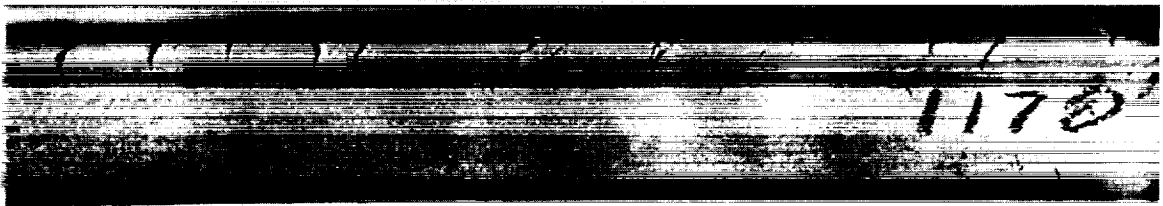


1145B

- (b) Heat V-12, vacuum-induction melted with 0.0089 percent B, less than 0.01 percent Zr, 0.0017 percent O, and 0.001 percent N.



- (c) Heat V-25, vacuum-induction melted with 0.0060 percent B, 0.06 percent Zr, 0.0037 percent O, and 0.002 percent N.



- (d) Heat V-Arc, vacuum-arc melted with 0.0006 percent B, 0.015 percent Zr, 0.0022 percent O, and 0.004 percent N.

L-59-1935

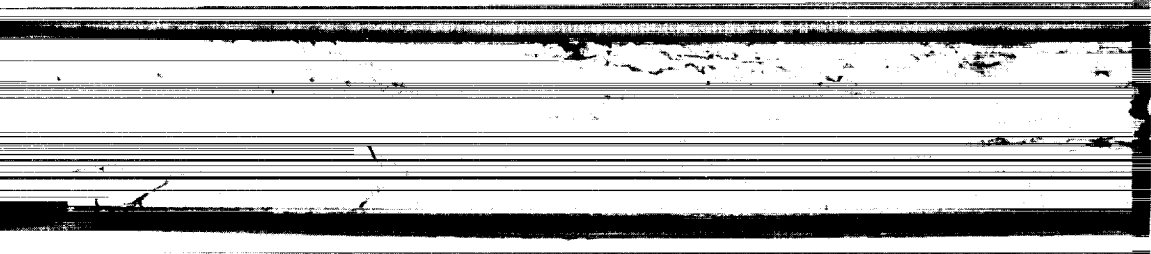
Figure 2.- Surface cracking as influenced by melting conditions and trace elements.



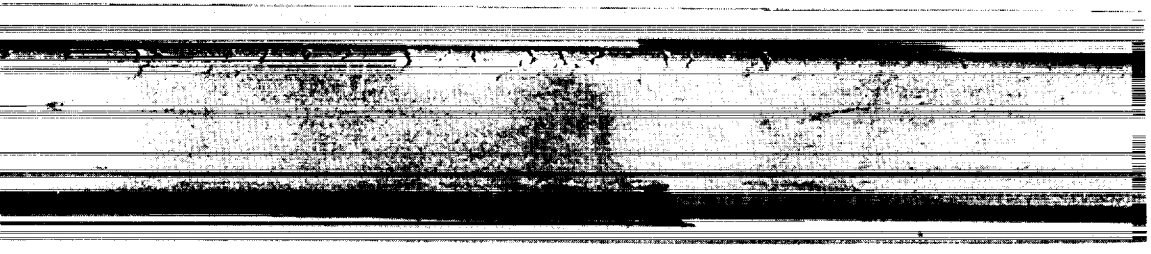


1159

(e) Heat A-6, air-induction melted with 0.0058 percent B, less than 0.01 percent Zr, 0.0050 percent O, and 0.028 percent N.



(f) Heat A-3, air-induction melted with 0.0096 percent B, 0.08 percent Zr, 0.0043 percent O, and 0.030 percent N.



(g) Heat V + Air, Vacuum + air-induction melted with 0.0090 percent B, less than 0.01 percent Zr, 0.0084 percent O, and 0.055 percent N.

L-59-1936

Figure 2.- Concluded.

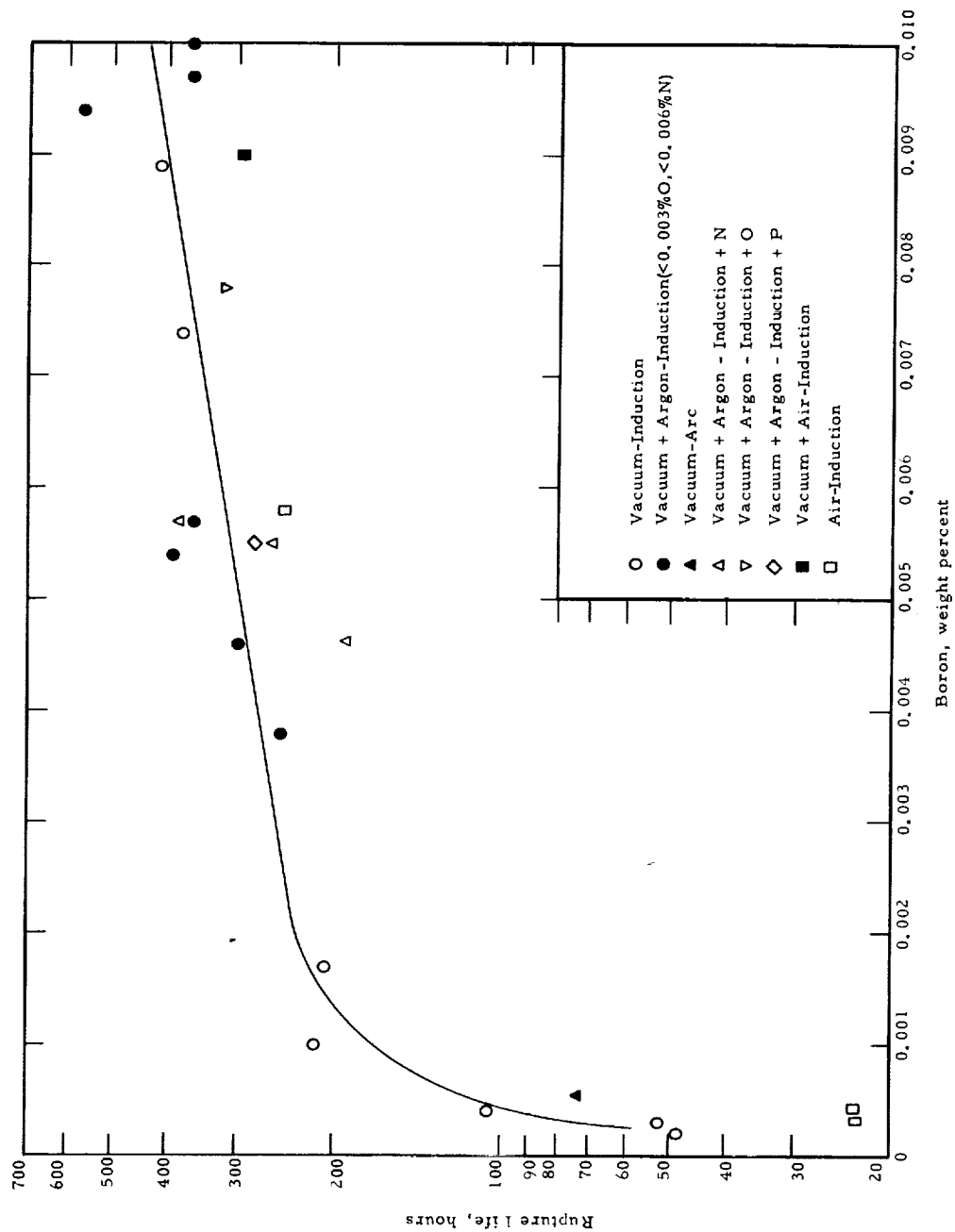


Figure 3.- Effect of boron on average rupture life at 1,600°F and 25,000 psi of heats with <0.01 percent Zr. Curve based on vacuum- or vacuum plus argon-induction heats with <0.003 percent O and <0.006 percent N.

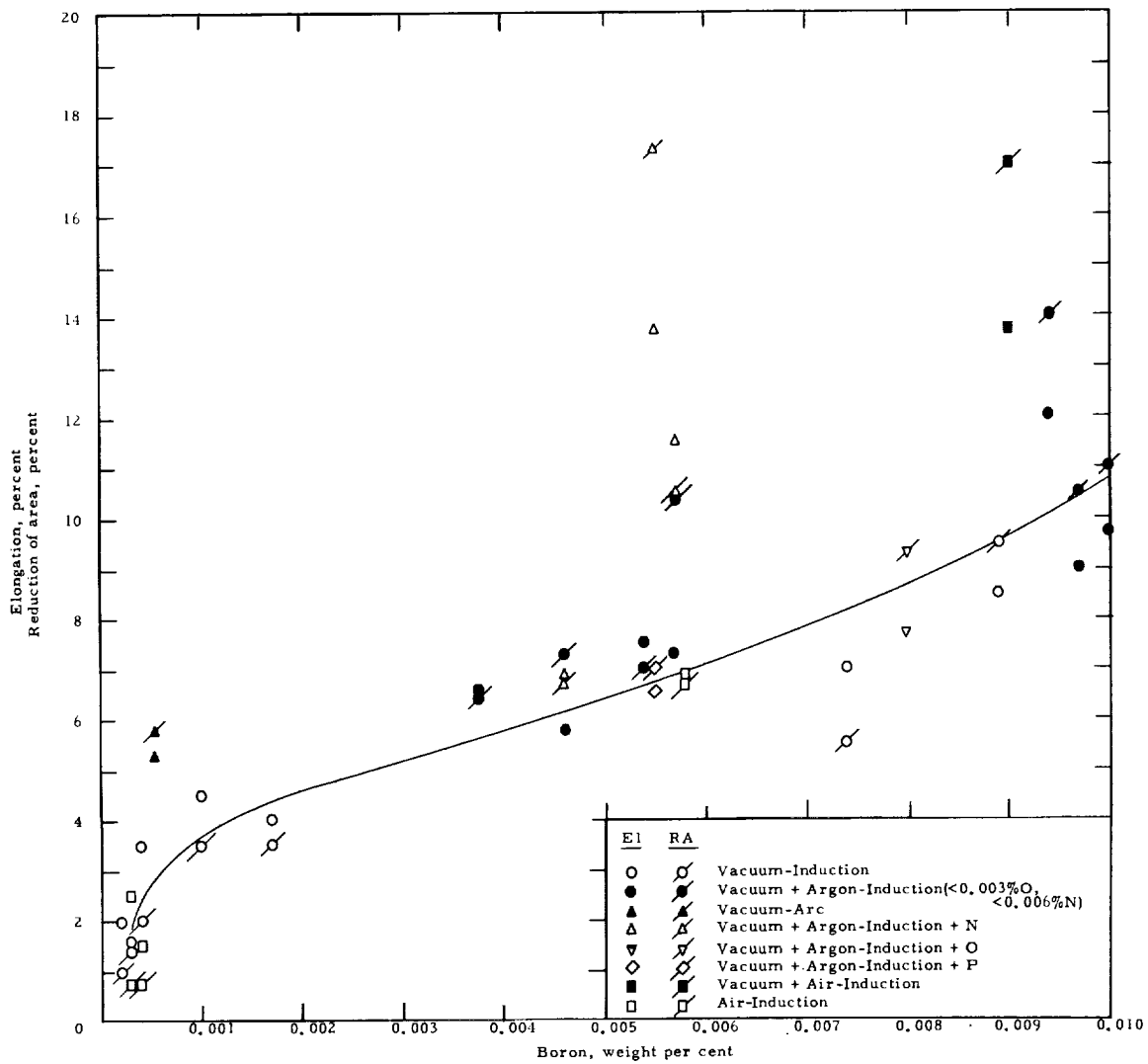


Figure 4.- Effect of boron on average ductility at 1,600° F and 25,000 psi of heats with <0.01 percent Zr. Curve based on vacuum- or vacuum plus argon-heats with <0.003 percent and <0.006 percent N.

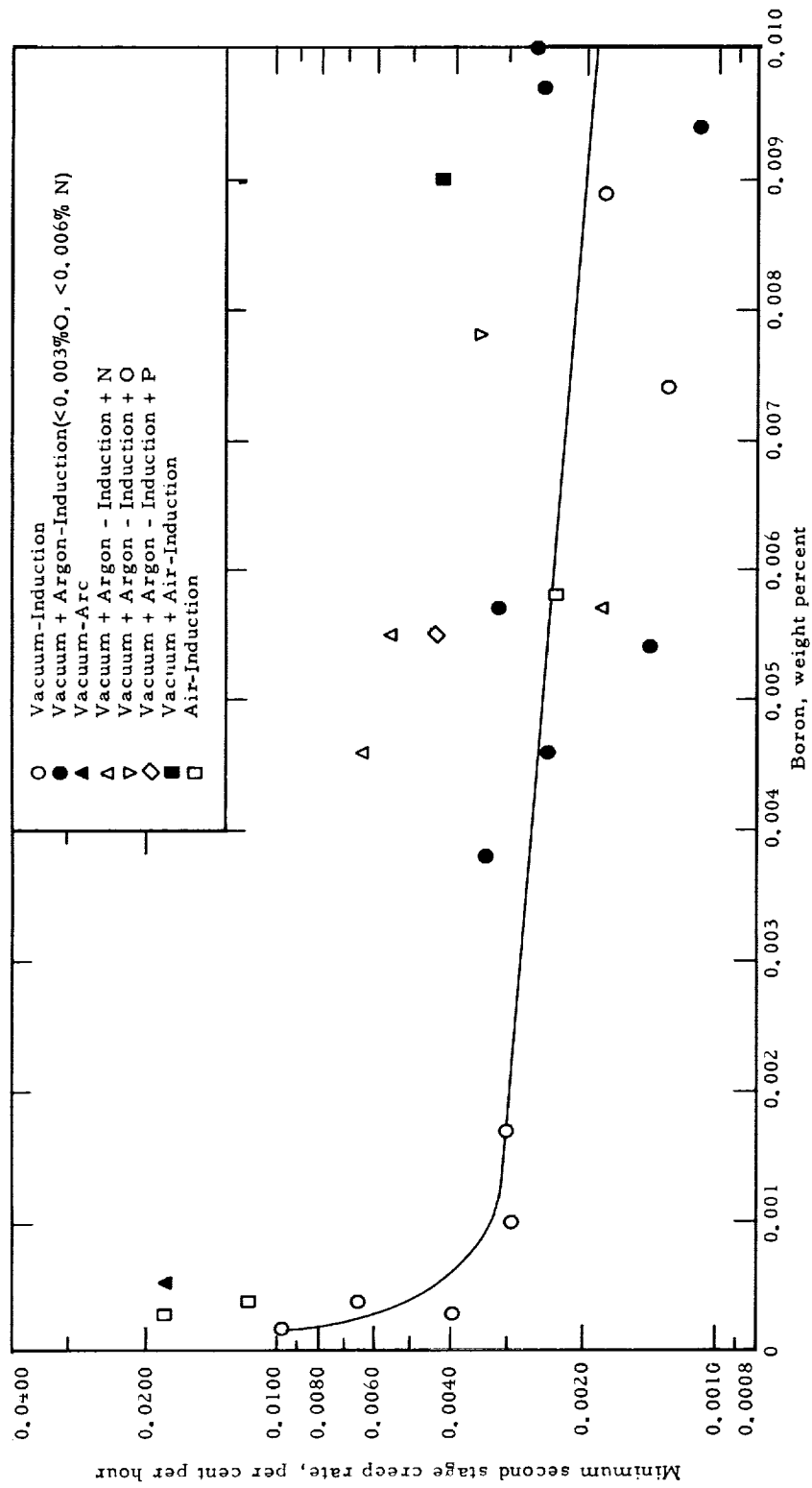


Figure 5.- Effect of boron content on average minimum second stage creep rate at 1,600° F and 25,000 psi of heats with <0.01 percent Zr. Curve based on vacuum- or vacuum plus argon-induction heats with <0.003 percent O and <0.006 percent N.

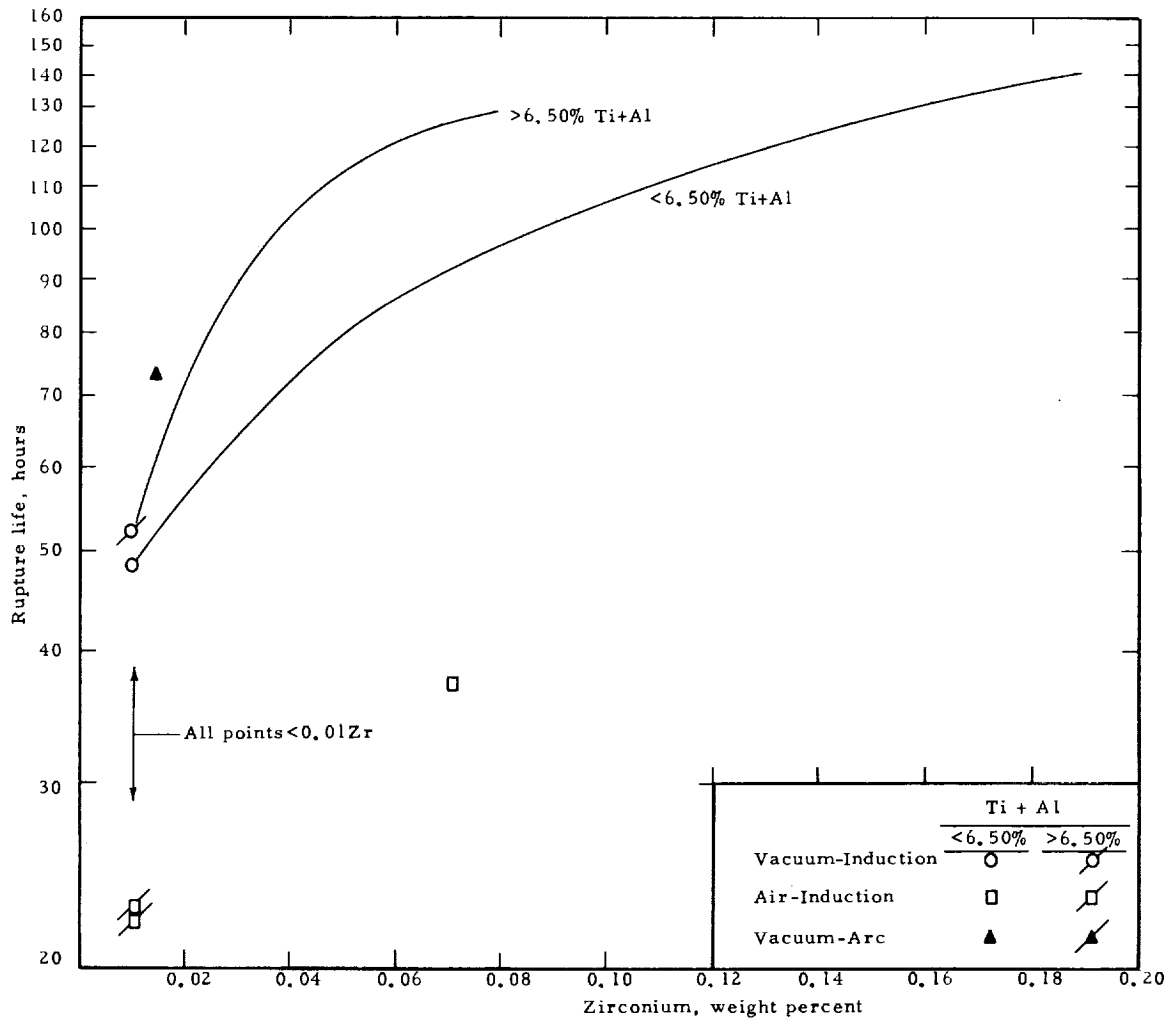


Figure 6.- Effect of zirconium content on average rupture life at  $1,600^{\circ}\text{F}$  and 25,000 psi for vacuum-induction heats with less than 0.0005 percent B (from ref. 1). Air-induction heats are plotted for comparison.

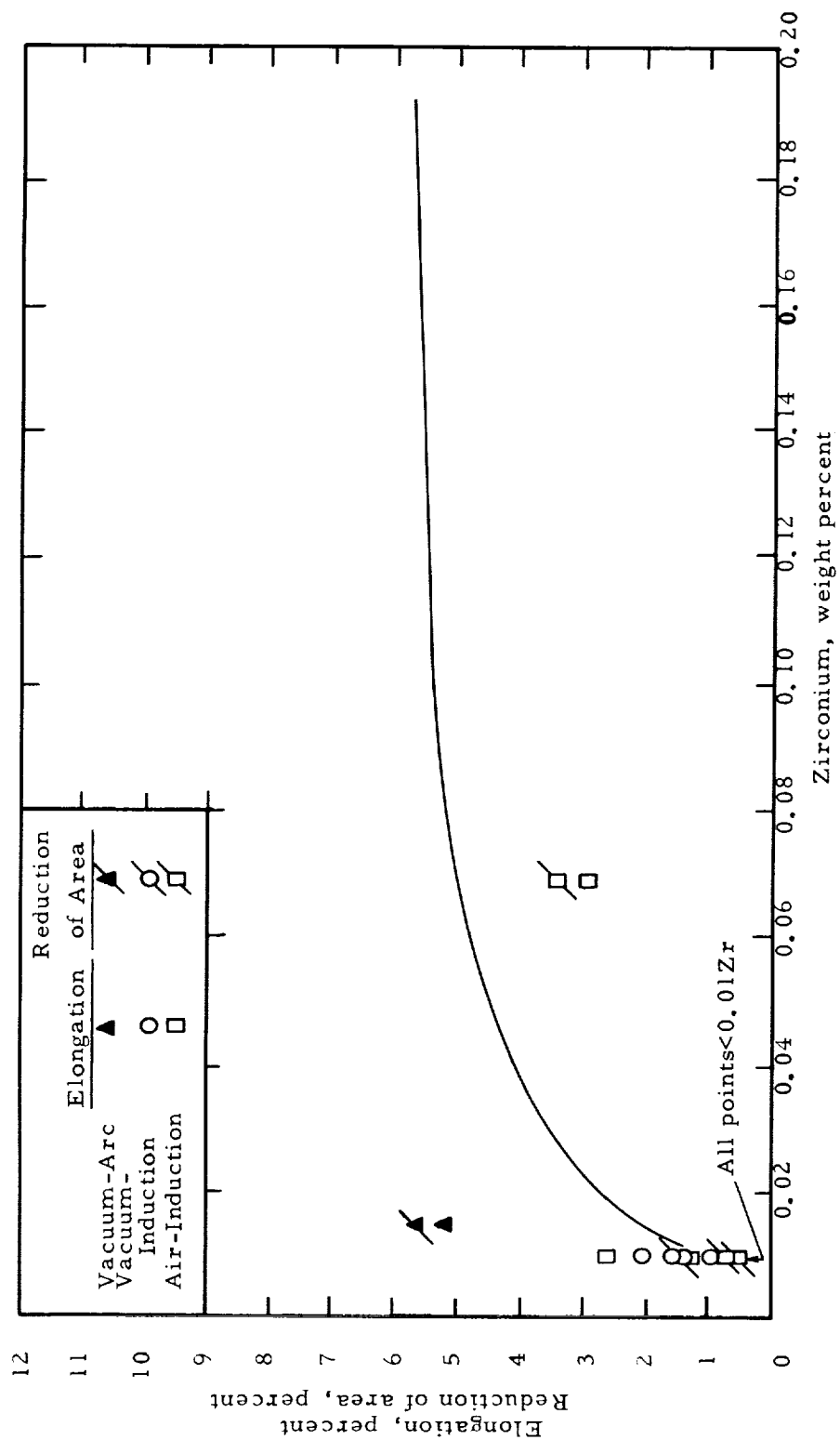


Figure 7.- Effect of zirconium content on average ductility at 1,600° F and 25,000 psi for vacuum-induction heats with <0.0005 percent B (from ref. 1). Air-induction heats are plotted for comparison.

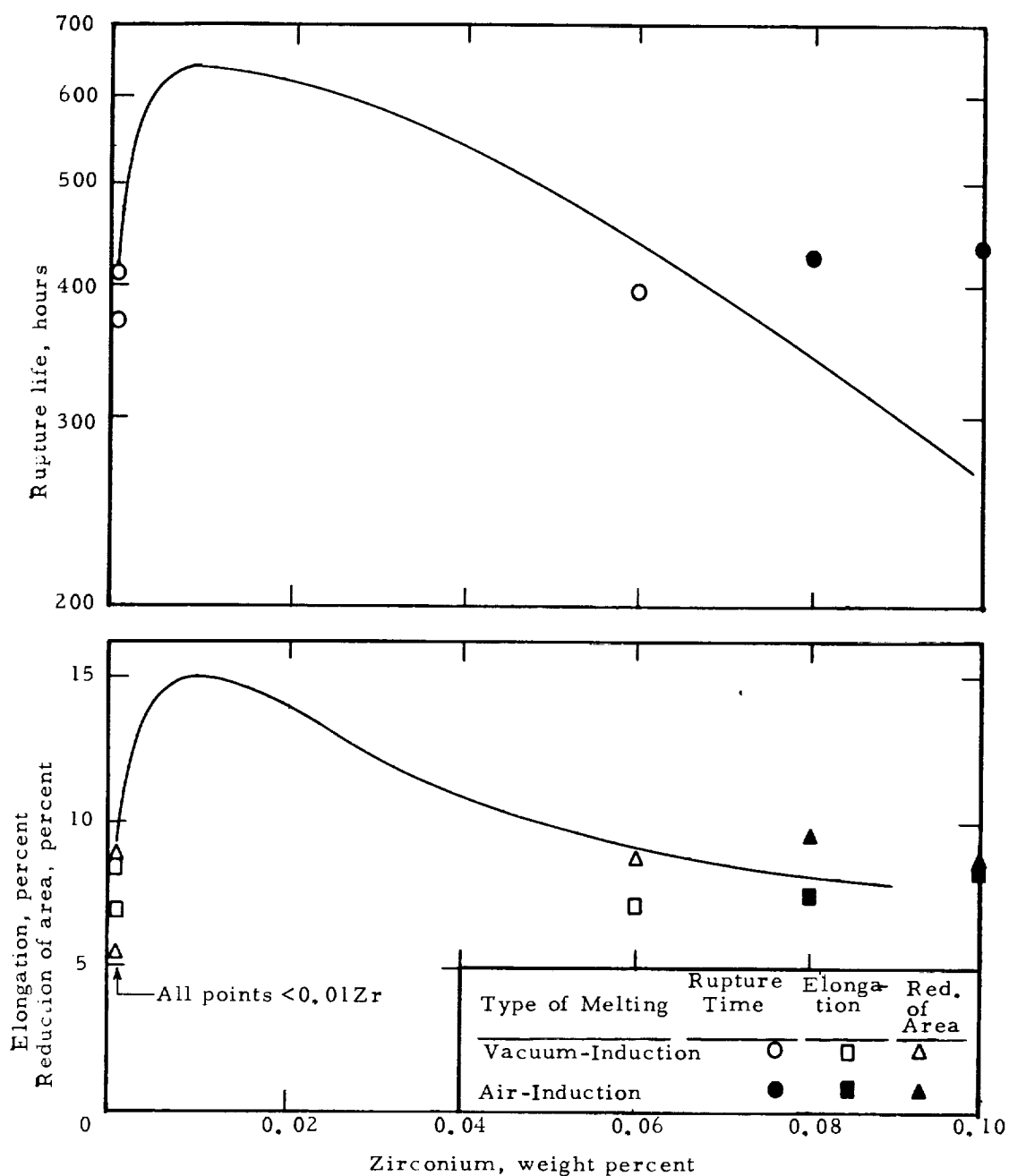


Figure 8.- Effect of zirconium content on average rupture life, elongation and reduction of area at 1,600° F and 25,000 psi for vacuum-induction heats with 0.0069 - 0.0090 percent B (from ref. 1). Air-induction heats are plotted for comparison.

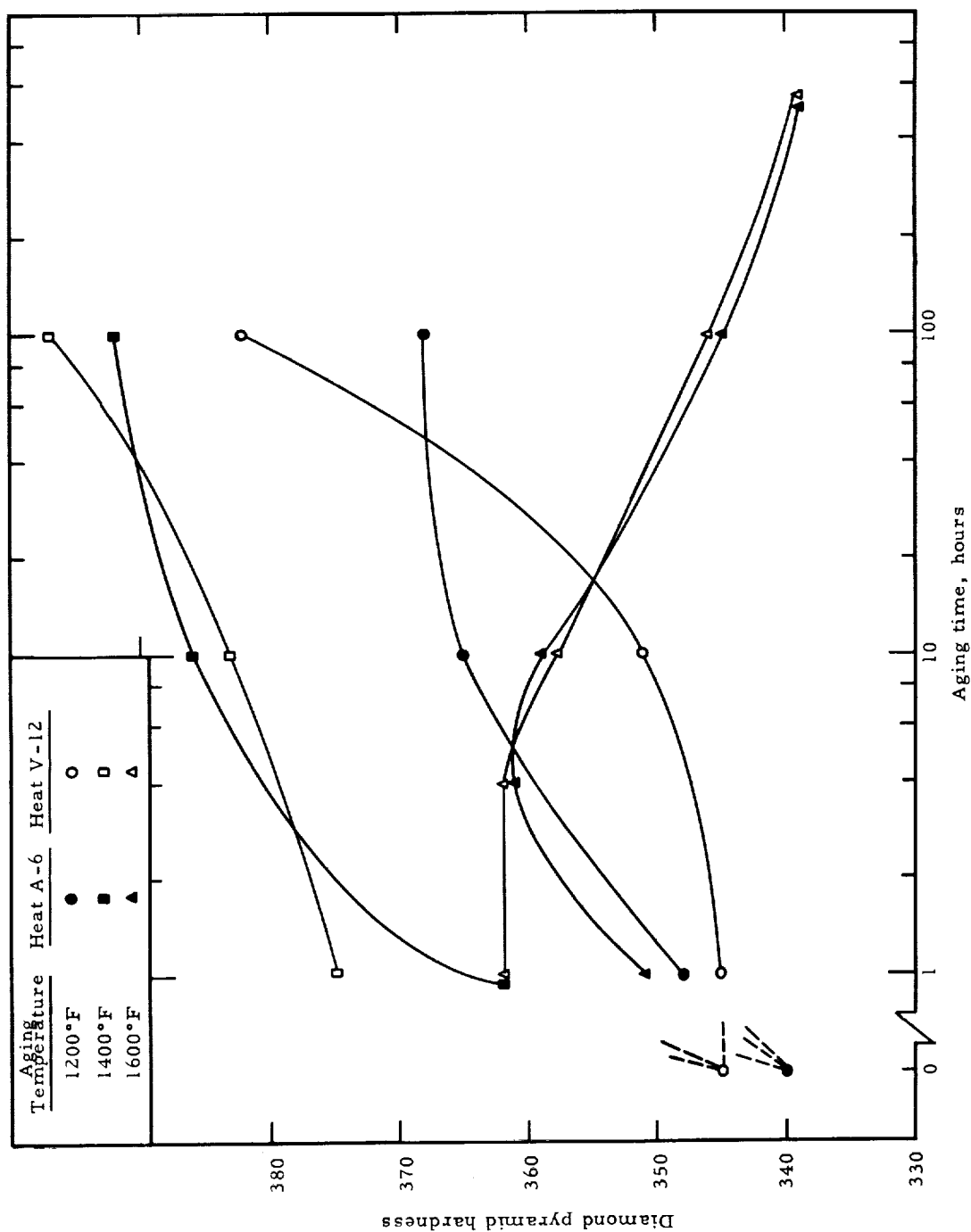
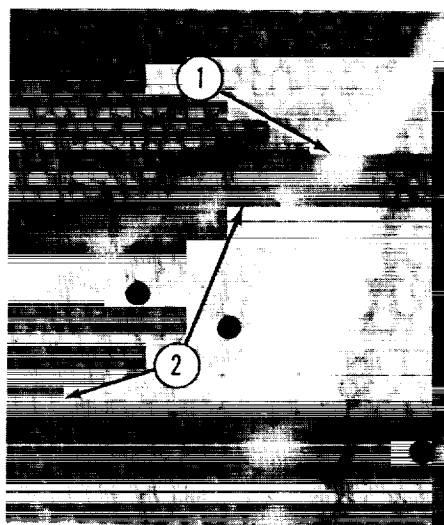
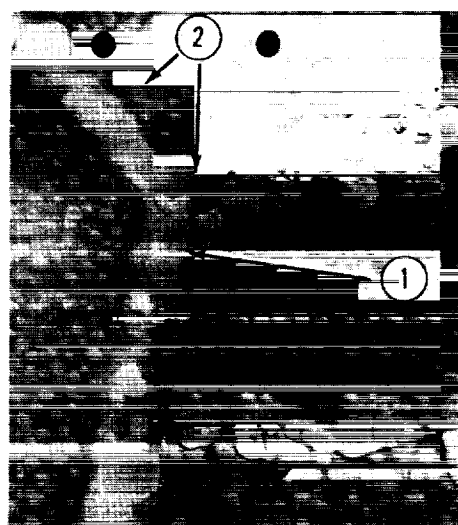


Figure 9.- Effect of aging on hardness of air- and vacuum-induction heats.



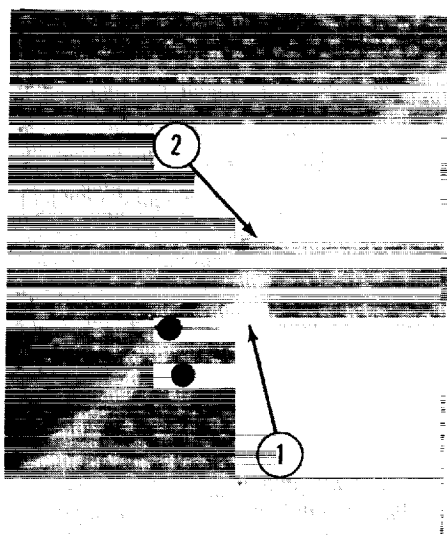


Heat V-12

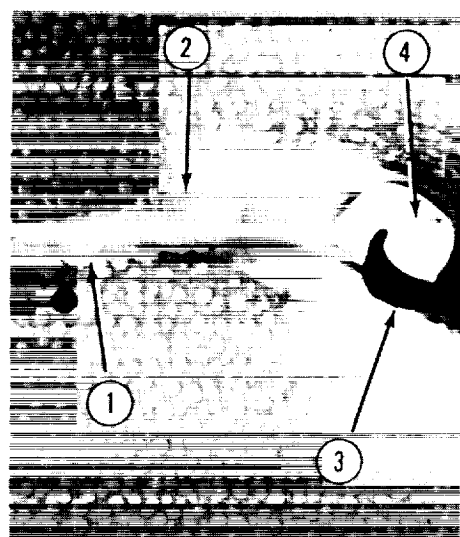


Heat A-6

(a) Aged 190 hours at 1,600° F.



Heat V-12; 28,000 psi, 188 hours

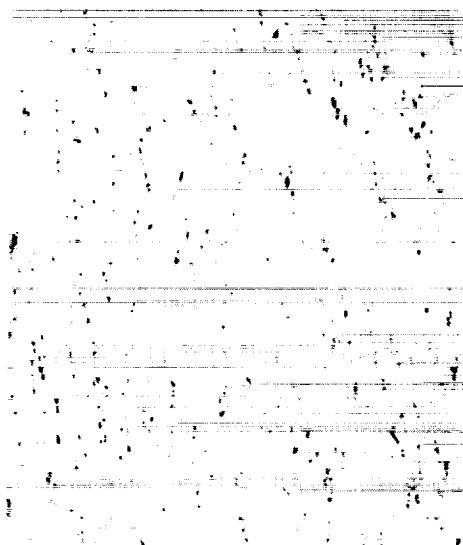


Heat A-6; 27,000 psi, 147 hours

(b) Stress-aged to give 1.2-percent creep deformation at 1,600° F. L-59-1937

Figure 10.- Electron micrographs of Heat V-12 and Heat A-6. X12,000.

① -Intergranular  $M_{23}C_6$ ; ② - $\gamma'$ ; ③ -microcrack; ④ -TiN.



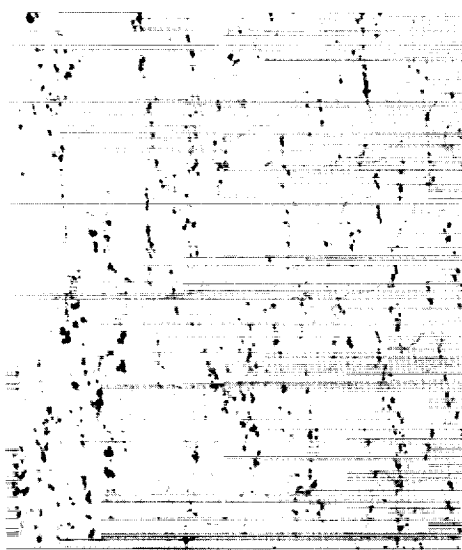
X100

(a) Heat V + Arg-7; 0.0015



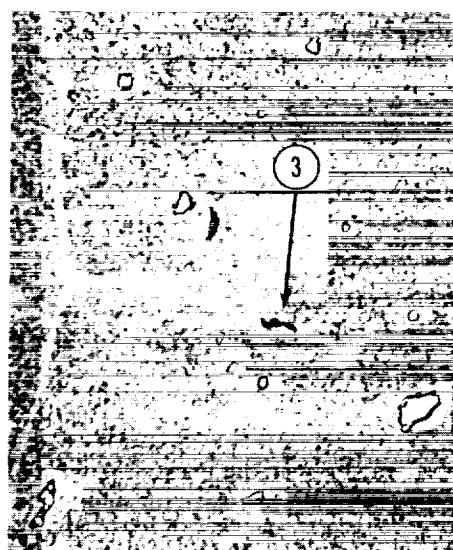
X1,000

nt 0 and 0.004 percent N.



X100

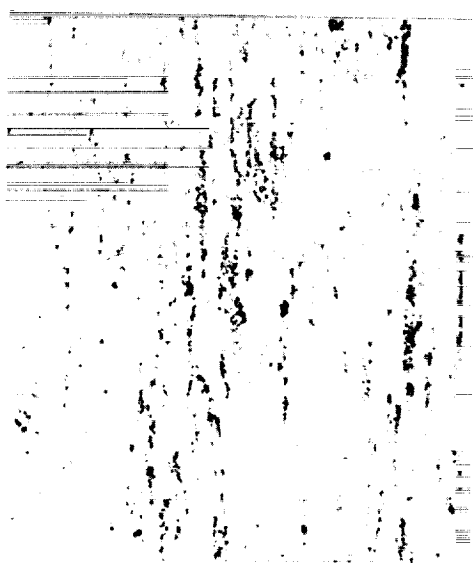
(b) Heat V + Arg-4 (O); 0.0080 percent O and 0.005 percent N.



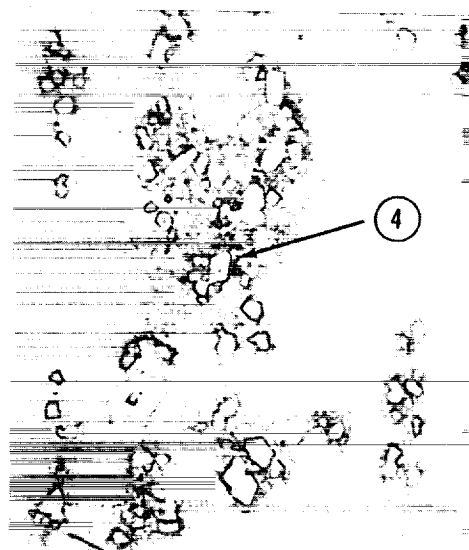
X1,000

L-59-1938

Figure 11.- Microstructures after 2-percent creep deformation at 1,600° F in 240 hours. ③ -microcrack; ④ -TiN.

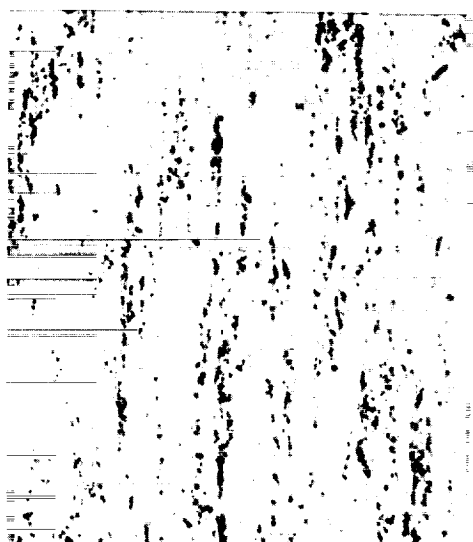


X100

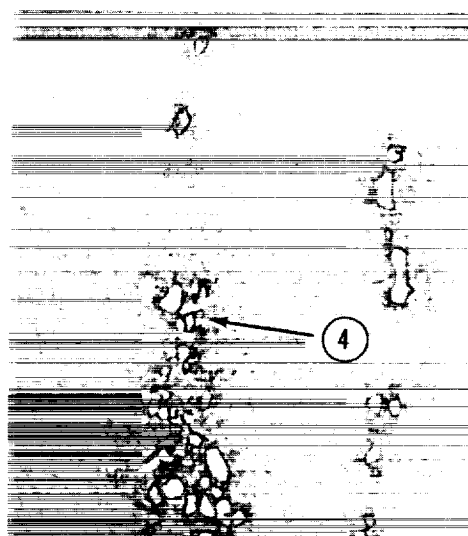


X1,000

(c) Heat V + Arg-9 (N); 0.0051 percent O and 0.048 percent N.



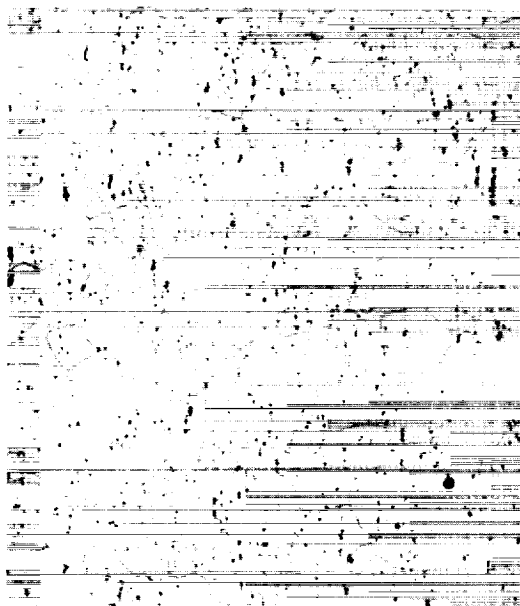
X100



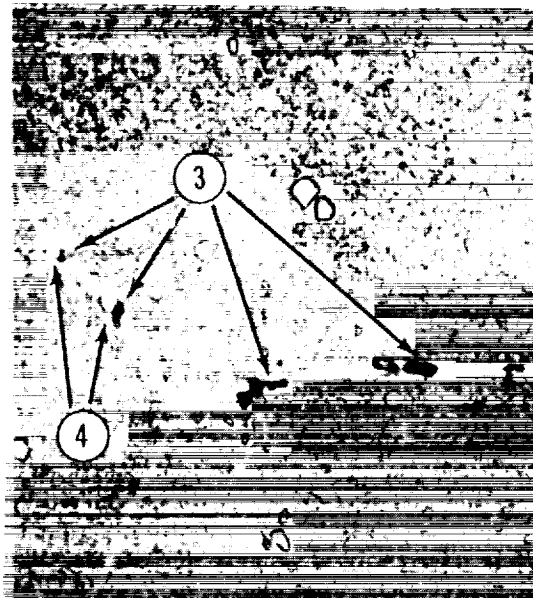
X1,000

(d) Heat V + Air; 0.0084 percent O and 0.055 percent N. L-59-1939

Figure 11.- Continued.



X100



X1,000

(e) Heat A-6; 0.0050 percent O and 0.028 percent N. L-59-1940

Figure 11.- Concluded.

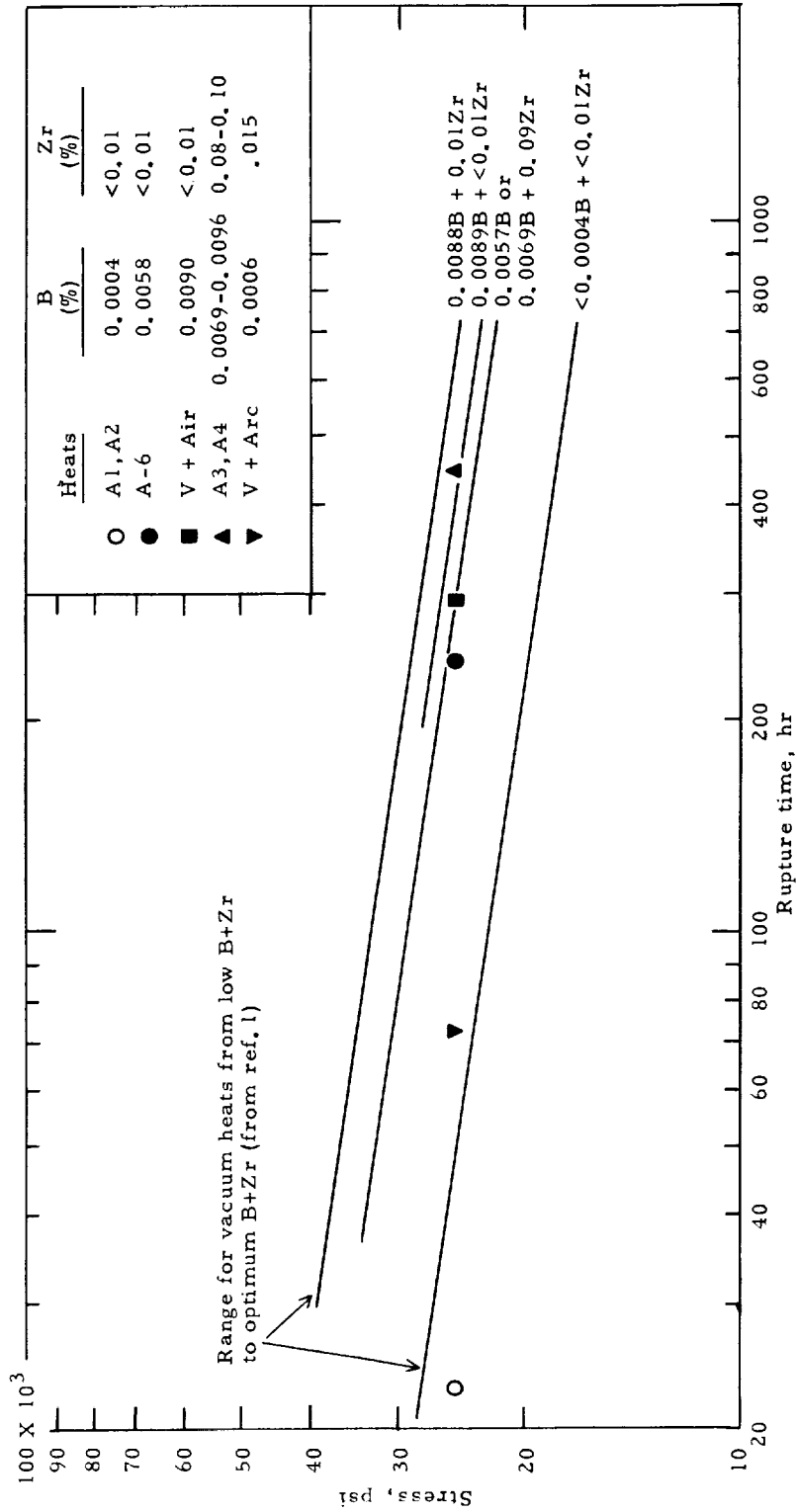


Figure 12.- Rupture times for heats melted in air or by the vacuum-arc process compared with approximate stress-rupture time curves at 1,600° F for vacuum heats with equivalent boron and zirconium contents.

